CHAPTER IV

RESULTS AND DISCUSSION

1. Determination of chitosan effects on protein profiles of rice seedlings after chitosan application

1.1 Proteome profiling of chitosan-responsive proteins in 'LTP123' rice

Oligomeric chitosan used in study previous showed the plant growth induction ability in 'LPT123' rice both normal condition (data not showed) and drought stress condition (Pongprayoon *et al.*, 2013). To elucidate the proteome response, total protein of rice seedlings treated with chitosan O80 at 40 mg/L were extracted and fractionated on 12.5% polyacrylamide gels one-dimensional electrophoresis (1-DE) (see in Fig. B2, Appendix B). Base on 1-DE coupled with LC-MS/MS analysis, total 3373 MASCOT-predicted proteins were found in rice leaf tissues. After cut-off the missing data, total 352 leaf proteins (see protein list in Appendix B) were collected and subjected to MEV software to analyze the differential expression in comparison between chitosan and control treatment.

Hierarchical clustering was accomplished for protein expression profiles. Of the total proteins, 105 significantly differently expressed proteins were classified into 12 groups according to their gene ontology (GO) provided in rice genome annotation project. The protein categories consisted of metabolic process (25%), signal transduction (18%), transcription (18%), transport (6%), photosynthesis (5%), translation (4%), defense response (2%), developmental process (2%), ATPase (1%), DNA repair (1%), ROS scavenging system (1%), and unknown (18%) as shown in Fig. 4.1.

All of significantly differentially expressed proteins were up-regulated as shown in Table 4.1 and by the heat map in Fig. 4.2. The heat map color indicates the level of protein expression in each biological replicate ranging from green (low expression) to red (high expression). Each column referred to three independent biological replicates. Major groups of known proteins were metabolic process (including carbohydrate, lipid, and protein metabolism as well as protein modification), signal transduction and transcription process.

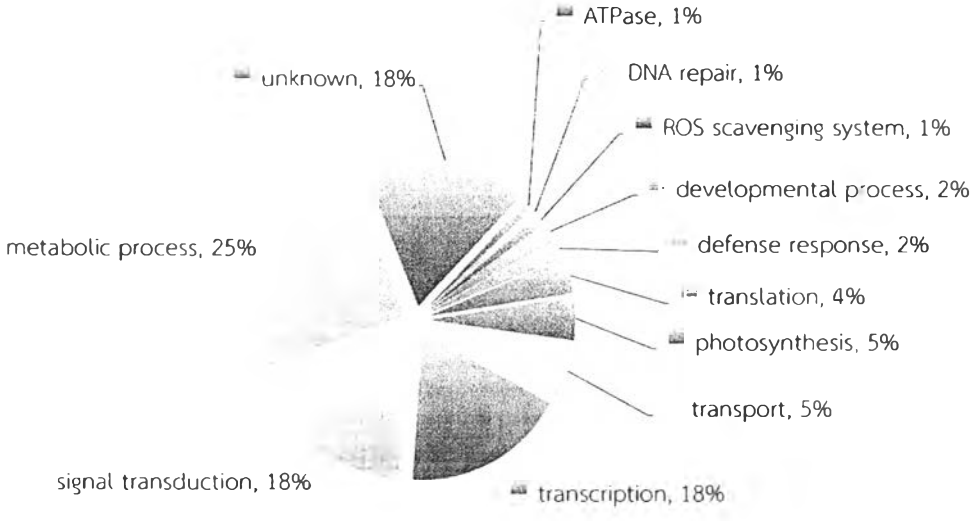

Figure 4.1 Functional categories of significantly differently expressed proteins in 'LPT123' rice leaves responsible for chitosan O80 at 40 mg/L. The given functions were retrieved from GO provided in rice genome annotation project.

Table 4.1 List of significantly differentially expressed proteins in 'LPT123' rice leaves responsible for chitosan O80 at 40 mg/L. The data were analyzed by MEV software ($p<0.05$)

LOC	Description[a]	Function[b]	Peptide[c]	ID Score[d]
LOC_Os11g47970	AAA-type ATPase family protein	ATPase	VPLILGIWGGK	53.86
LOC_Os01g61880	Respiratory burst oxidase	defense response	TTSSLAR	16.02
LOC_Os10g25487	NBS-LRR disease resistance protein	defense response	LPSSIIK	11.82
LOC_Os10g09990	Cytokinin-O-glucosyltransferase 3	developmental process	HVGAQ	2.50
LOC_Os05g09620	SCC3	developmental process	ASGSNS	8.21
LOC_Os01g49270	XPA-binding protein 2	DNA repair	AHAEAR	12.56
LOC_Os01g74000	Glycerol-3-phosphate dehydrogenase	metabolic process	AAIMR	7.31
LOC_Os04g16680	Fructose-1,6-bisphosphatase	metabolic process	GIFTNVTSPTAK	32.14
LOC_Os04g38600	Glyceraldehyde-3-phosphate dehydrogenase	metabolic process	VIAWYDNEWGYSQR	87.70
LOC_Os07g47120	Beta-amylase	metabolic process	CGAVR	12.94
LOC_Os02g15230	GDSL-like lipase/acylhydrolase	metabolic process	MGAVR	13.15
LOC_Os04g55060	3-oxoacyl-synthase III, chloroplast precursor	metabolic process	GGGIR	12.13
LOC_Os01g11300	Cytochrome P450	metabolic process	AEPIR	6.70
LOC_Os01g66180	Cytochrome C	metabolic process	AAGHK	11.44
LOC_Os03g14450	Enolase	metabolic process	VNQIGSVTESIEAVK	93.79
LOC_Os03g18640	Laccase precursor protein	metabolic process	ATFGLEK	14.30
LOC_Os04g16740	ATP synthase subunit alpha	metabolic process	IAQIPVSEAYLGR	33.60
LOC_Os04g20260	UDP-glucoronosyl and UDP-glucosyl transferase	metabolic process	DGAMSHQLR	9.65
LOC_Os05g41640	Phosphoglycerate kinase protein	metabolic process	FLKPSVAGFLLQK	23.43
LOC_Os07g44840	Bacterial transferase hexapeptide domain containing protein	metabolic process	GTGQAMDRLGSTI QGGLR	5.45
LOC_Os08g01150	DTA2	metabolic process	MRGSSNNHK	15.34
LOC_Os08g39694	Cytochrome P450	metabolic process	GGPAHR	23.52
LOC_Os10g08550	Enolase	metabolic process	LAMQEFMILPTGAA SFK	44.03
LOC_Os10g11140	Phosphoglucomutase	metabolic process	DKPTVIT	19.89
LOC_Os10g31780	Oxidoreductase, short chain dehydrogenase/reductase family domain containing protein	metabolic process	IPAGAGGR	11.90

[a] protein descriptions retrieved from rice genome annotation project

[b] protein function retrieved from GO provided in rice genome annotation project

[c] predicted peptides analyzed by LC-MS/MS analysis

[d] ID score obtained from MASCOT

Table 4.1 (cont.) List of significantly differentially expressed proteins in 'LPT123' rice leaves responsible for chitosan O80 at 40 mg/L. The data were analyzed by MEV software (p<0.05)

LOC	Description[a]	Function[b]	Peptide[c]	ID Score[d]
LOC_Os11g26850	Erythronate-4-phosphate dehydrogenase	metabolic process	IVLTIIR	43.24
LOC_Os02g17360	PPR repeat domain containing protein	metabolic process	AAEGAGAK	13.09
LOC_Os03g52070	OsSCP20 - Putative Serine Carboxypeptidase homologue	metabolic process	LQGYIVGNPITGSK	13.32
LOC_Os03g58204	Ribosomal protein L4	metabolic process	NLPGVDVANVER	44.86
LOC_Os04g56400	Glutamine synthetase, catalytic domain containing protein	metabolic process	GCSIR	10.06
LOC_Os04g35680	U-box domain containing protein	metabolic process	APGGTR	14.17
LOC_Os08g32970	Annexin	metabolic process	CAESPAK	16.31
LOC_Os01g31690	Oxygen-evolving enhancer protein 1, chloroplast precursor	photosynthesis	VPFLFTIK	39.04
LOC_Os03g03720	Glyceraldehyde-3-phosphate dehydrogenase	photosynthesis	AVALVLPQLK	41.91
LOC_Os09g17740	Chlorophyll A-B binding protein	photosynthesis	FGEAVWFK	49.36
LOC_Os12g17600	Ribulose bisphosphate carboxylase small chain, chloroplast precursor	photosynthesis	XQVWPIEGIK	28.13
LOC_Os12g19381	Ribulose bisphosphate carboxylase small chain, chloroplast precursor	photosynthesis	LPMFGCTDATQVLK	62.22
LOC_Os12g08730	Thioredoxin	ROS scavenging system	SIPTVLMFK	24.69
LOC_Os02g21700	STE_MEKK_ste11_MAP3K.8	signal transduction	GTPMFLAPEAAR	19.86
LOC_Os02g39970	Regulatory subunit	signal transduction	GAVCSR	3.85
LOC_Os03g15770	Tyrosine protein kinase domain containing protein	signal transduction	VAGTM	4.60
LOC_Os03g49510	Phosphatidylinositol-4-phosphate 5-kinase	signal transduction	DSVYER	12.62
LOC_Os03g53100	Response regulator receiver domain containing protein	signal transduction	TTVVSR	21.69
LOC_Os04g52840	Tyrosine protein kinase domain containing protein	signal transduction	SSNMR	7.28
LOC_Os06g47680	OsFBX205 - F-box domain containing protein	signal transduction	TTVVSR	21.69
LOC_Os06g47740	Phytosulfokine receptor precursor	signal transduction	VFSAGR	4.40

[a] protein descriptions retrieved from rice genome annotation project

[b] protein function retrieved from GO provided in rice genome annotation project

[c] predicted peptides analyzed by LC-MS/MS analysis

[d] ID score obtained from MASCOT

Table 4.1 (cont.) List of significantly differentially expressed proteins in 'LPT123' rice leaves responsible for chitosan O80 at 40 mg/L. The data were analyzed by MEV software (p<0.05)

LOC	Description[a]	Function[b]	Peptide[c]	ID Score[d]
LOC_Os08g25380	Serine/threonine-protein kinase BRI1-like 1 precursor	signal transduction	HGSPR	12.12
LOC_Os08g31060	Phospholipase D alpha 1	signal transduction	DGRMGAAR	11.45
LOC_Os08g39550	Polygalacturonase inhibitor 2 precursor	signal transduction	LTGEIPR	20.11
LOC_Os09g02729	Phospholipase C	signal transduction	GAAGSGR	16.56
LOC_Os09g13820	Pollen signalling protein with adenylyl cyclase activity	signal transduction	CNNSVS	2.96
LOC_Os09g36520	KI1 protein	signal transduction	ARVDGAA	10.12
LOC_Os10g02720	OsWAK99 - OsWAK receptor-like protein kinase	signal transduction	VIVGK	17.96
LOC_Os10g25010	OsCML8 - Calmodulin-related calcium sensor protein	signal transduction	MSTVK	8.80
LOC_Os11g10340	OsFBX417 - F-box domain containing protein	signal transduction	LDADKER	27.67
LOC_Os12g31610	Lectin-like protein kinase	signal transduction	SGLRGCDAR	10.24
LOC_Os12g39120	Protein phosphatase 2C	signal transduction	AALTEAAR	28.21
LOC_Os01g04800	B3 DNA binding domain containing protein	transcription	MTVSDIGK	6.50
LOC_Os01g11120	CID11	transcription	AAVAGGSR	14.64
LOC_Os01g38710	Nucleic acid binding protein	transcription	TAADDK	4.73
LOC_Os01g50040	DNA binding protein	transcription	PAAKR	10.41
LOC_Os01g63160	MYB family transcription factor	transcription	GIPGR	10.98
LOC_Os02g52960	PHD-finger domain containing protein	transcription	ARAEGLPEGAAPGV GVDLYAQAR	10.80
LOC_Os03g02240	AT-GTL1	transcription	RGGGGIGGGGGGGK	6.86
LOC_Os03g27030	RNA recognition motif containing protein	transcription	TVDGR	15.09
LOC_Os03g45450	WRKY60	transcription	GAGGGR	17.35
LOC_Os03g60130	Transcription elongation factor protein	transcription	GGAPK	6.78
LOC_Os07g44030	MYB/SANT domain protein	transcription	QPNHSGK	25.16
LOC_Os08g05510	MYB family transcription factor	transcription	ADPPAEK	8.05
LOC_Os08g28214	Tesmin/TSO1-like CXC domain containing protein	transcription	NPAAFMPK	5.46
LOC_Os08g44910	DNA binding protein	transcription	STTFR	7.37

[a] protein descriptions retrieved from rice genome annotation project

[b] protein function retrieved from GO provided in rice genome annotation project

[c] predicted peptides analyzed by LC-MS/MS analysis

[d] ID score obtained from MASCOT

Table 4.1 (cont.) List of significantly differentially expressed proteins in 'LPT123' rice leaves responsible for chitosan O80 at 40 mg/L. The data were analyzed by MEV software (p<0.05)

LOC	Description[a]	Function[b]	Peptide[c]	ID Score[d]
LOC_Os09g32010	Ternary complex factor MIP1	transcription	YVVHR	13.99
LOC_Os10g30054	ENT domain containing protein	transcription	AMVPDK	17.55
LOC_Os10g30719	MYB family transcription factor	transcription	GKAQK	10.86
LOC_Os11g48000	ZOS11-11 - C2H2 zinc finger protein	transcription	AVVHA	11.39
LOC_Os12g31430	Helix-loop-helix DNA-binding domain containing protein	transcription	ATIPAR	11.31
LOC_Os04g28180	Ribosomal protein	translation	GKGAAA	10.22
LOC_Os05g47630	Peptidyl-tRNA hydrolase, mitochondrial precursor protein	translation	SMVGK	15.60
LOC_Os06g43760	tRNA synthetase class I	translation	GRHVSR	5.82
LOC_Os09g34070	RNA recognition motif containing protein	translation	GYGVR	4.08
LOC_Os01g12680	C4-dicarboxylate transporter/malic acid transport protein	transport	DGAPR	9.78
LOC_Os03g08070	Copper-transporting ATPase PAA1	transport	SHTGFML	14.13
LOC_Os04g41320	Nucleotide-sugar transporter family protein	transport	KPLLPI	23.47
LOC_Os07g01920	Nucleolar GTP-binding protein 1	transport	SSIGK	16.46
LOC_Os09g03750	Ankyrin	transport	TASTR	17.70
LOC_Os09g15330	Transporter family protein	transport	LIAASPR	11.27
LOC_Os01g27030	Hypothetical protein	unknown	VAAHK	11.27
LOC_Os01g56530	Lateral organ boundaries domain protein 18-like	unknown	GAAEFAAVHR	21.39
LOC_Os02g28580	Unknown protein	unknown	NIVDGPK	9.67
LOC_Os03g23970	Diphthine synthase	unknown	IVAGPMK	8.69
LOC_Os03g29420	Hypothetical protein	unknown	EGRPW	14.28
LOC_Os03g38740	CAF protein-like	unknown	DLIAGHK	15.21
LOC_Os04g34600	Abscisic stress-ripening	unknown	KHHLFG	18.60
LOC_Os04g52950	Nitrate-induced NOI protein	unknown	MTTMDK	9.89
LOC_Os06g07470	Unknown protein	unknown	DAGIFR	24.09
LOC_Os08g17820	Putative diaphanous 1	unknown	LPGMRGR	5.84
LOC_Os09g15560	OsFBX314 - F-box domain containing protein	unknown	GGLLLLSKK	15.55

[a] protein descriptions retrieved from rice genome annotation project

[b] protein function retrieved from GO provided in rice genome annotation project

[c] predicted peptides analyzed by LC-MS/MS analysis

[d] ID score obtained from MASCOT

Table 4.1 (cont.) List of significantly differentially expressed proteins in 'LPT123' rice leaves responsible for chitosan O80 at 40 mg/L. The data were analyzed by MEV software ($p<0.05$)

LOC	Description[a]	Function[b]	Peptide[c]	ID Score[d]
LOC_Os09g37510	DUF292 domain containing protein	unknown	MMATAGSK	11.78
LOC_Os11g05550	Unknown protein	unknown	MAADGGALK	12.59
LOC_Os11g06720	Abscisic stress-ripening	unknown	KHHLFG	19.21
LOC_Os11g11730	Unknown protein	unknown	DAIAAVQECK	10.49
LOC_Os11g18070	HGWP repeat containing protein-like	unknown	DIIIFR	29.39
LOC_Os11g42100	Leucine rich repeat family protein	unknown	ACLNAGR	16.72
LOC_Os11g42940	Integral membrane protein	unknown	MDGAAR	9.99
LOC_Os12g02050	Unknown protein	unknown	MENTSSGK	12.76

[a] protein descriptions retrieved from rice genome annotation project

[b] protein function retrieved from GO provided in rice genome annotation project

[c] predicted peptides analyzed by LC-MS/MS analysis

[d] ID score obtained from MASCOT

Figure 4.2 (next page) Hierarchical clustering of significantly differently expressed proteins in 'LPT123' rice leaves responsible for chitosan O80 at 40 mg/L. Each column indicated independent biological replication. The color ranging from green-black-red indicated the level of protein expression (green: low, black: middle, and red: high).

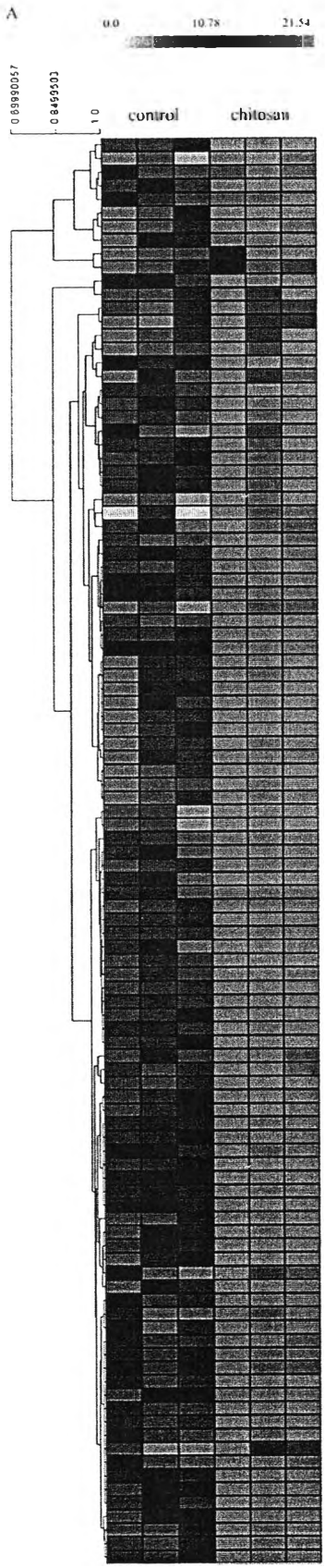

locus	description
LOC_Os11g47970	AAA-type ATPase family protein
LOC_Os04g16680	fructose-1,6-bisphosphatase
LOC_Os01g38710	nucleic acid binding protein
LOC_Os12g31430	helix-loop-helix DNA-binding domain containing protein
LOC_Os04g28180	ribosomal protein
LOC_Os10g25010	OsCML8 - Calmodulin-related calcium sensor protein
LOC_Os01g63160	MYB family transcription factor
LOC_Os07g01920	nucleolar GTP-binding protein 1
LOC_Os03g52070	OsSCP20 - Putative Serine Carboxypeptidase homologue
LOC_Os09g15560	OsFBX314 - F-box domain containing protein
LOC_Os01g61880	respiratory burst oxidase
LOC_Os06g47740	phytosulfokine receptor precursor
LOC_Os03g02240	AT-GTL1
LOC_Os11g11730	unknown protein
LOC_Os12g08730	thioredoxin
LOC_Os03g60130	transcription elongation factor protein
LOC_Os01g50040	DNA binding protein
LOC_Os02g28580	unknown protein
LOC_Os04g55060	3-oxoacyl-synthase III, chloroplast precursor
LOC_Os04g56400	glutamine synthetase, catalytic domain containing protein
LOC_Os08g31060	phospholipase D alpha 1
LOC_Os02g52960	PHD-finger domain containing protein
LOC_Os10g09990	cytokinin-O-glucosyltransferase 3
LOC_Os04g38600	glyceraldehyde-3-phosphate dehydrogenase
LOC_Os12g39120	protein phosphatase 2C
LOC_Os03g23970	diphthine synthase
LOC_Os12g31610	lectin-like protein kinase
LOC_Os04g52840	tyrosine protein kinase domain containing protein
LOC_Os09g34070	RNA recognition motif containing protein
LOC_Os11g26850	erythronate-4-phosphate dehydrogenase
LOC_Os09g36520	K11 protein
LOC_Os11g48000	ZOS11-11 - C2H2 zinc finger protein
LOC_Os03g15770	tyrosine protein kinase domain containing protein
LOC_Os08g44910	DNA binding protein
LOC_Os09g37510	DUF292 domain containing protein
LOC_Os03g03720	glyceraldehyde-3-phosphate dehydrogenase
LOC_Os05g47630	peptidyl-tRNA hydrolase, mitochondrial precursor protein
LOC_Os11g18070	HGWP repeat containing protein-like
LOC_Os01g31690	oxygen-evolving enhancer protein 1, chloroplast precursor
LOC_Os03g58204	ribosomal protein L4
LOC_Os05g41640	phosphoglycerate kinase protein
LOC_Os09g17740	chlorophyll A-B binding protein
LOC_Os08g25380	serine/threonine-protein kinase BRI1-like 1 precursor
LOC_Os03g27030	RNA recognition motif containing protein
LOC_Os06g43760	tRNA synthetase class I
LOC_Os11g05550	unknown protein
LOC_Os04g16740	ATP synthase subunit alpha
LOC_Os09g13820	pollen signalling protein with adenylyl cyclase activity
LOC_Os11g42940	integral membrane protein
LOC_Os12g17600	ribulose bisphosphate carboxylase small chain, chloroplast precursor
LOC_Os12g19381	ribulose bisphosphate carboxylase small chain, chloroplast precursor
LOC_Os08g05510	MYB family transcription factor
LOC_Os11g10340	OsFBX417 - F-box domain containing protein
LOC_Os08g28214	tesmin/TSO1-like CXC domain containing protein
LOC_Os01g11120	CID11
LOC_Os03g08070	copper-transporting ATPase PAA1
LOC_Os07g44030	MYB/SANT domain protein
LOC_Os10g30719	MYB family transcription factor
LOC_Os01g12680	C4-dicarboxylate transporter/malic acid transport protein
LOC_Os10g11140	phosphoglucomutase
LOC_Os09g15330	transporter family protein
LOC_Os03g38740	CAF protein-like
LOC_Os01g11300	cytochrome P450
LOC_Os04g52950	nitrate-induced NOI protein
LOC_Os04g35680	U-box domain containing protein
LOC_Os04g34600	abscisic stress-ripening
LOC_Os11g42100	leucine rich repeat family protein
LOC_Os09g32010	ternary complex factor MIP1
LOC_Os03g45450	WRKY60
LOC_Os10g30054	ENT domain containing protein
LOC_Os03g53100	response regulator receiver domain containing protein
LOC_Os06g47680	OsFBX205 - F-box domain containing protein
LOC_Os03g18640	laccase precursor protein
LOC_Os02g15230	GDSL-like lipase/acylhydrolase
LOC_Os10g02720	OsWAK99 - OsWAK receptor-like protein kinase
LOC_Os04g41320	nucleotide-sugar transporter family protein
LOC_Os08g32970	annexin
LOC_Os01g66180	cytochrome c
LOC_Os09g03750	ankyrin
LOC_Os03g14450	enolase
LOC_Os10g08550	enolase
LOC_Os08g39694	cytochrome P450
LOC_Os03g49510	phosphatidylinositol-4-phosphate 5-kinase
LOC_Os08g17820	putative diaphanous 1
LOC_Os11g06720	abscisic stress-ripening
LOC_Os01g49270	XPA-binding protein 2
LOC_Os01g04800	B3 DNA binding domain containing protein
LOC_Os01g27030	hypothetical protein
LOC_Os08g39550	polygalacturonase inhibitor 2 precursor
LOC_Os07g47120	beta-amylase
LOC_Os10g25487	NBS-LRR disease resistance protein
LOC_Os09g02729	phospholipase C
LOC_Os02g17360	PPR repeat domain containing protein
LOC_Os08g01150	DTA2
LOC_Os02g21700	MEKK
LOC_Os01g74000	glycerol-3-phosphate dehydrogenase
LOC_Os01g56530	lateral organ boundaries domain protein 18-like
LOC_Os05g09620	SCC3
LOC_Os10g31780	oxidoreductase, short chain dehydrogenase/reductase family domain containing protein
LOC_Os02g39970	regulatory subunit
LOC_Os06g07470	unknown protein
LOC_Os03g29420	hypothetical protein
LOC_Os07g44840	bacterial transferase hexapeptide domain containing protein.
LOC_Os04g20260	UDP-glucoronosyl and UDP-glucosyl transferase
LOC_Os12g02050	unknown protein

1.2 Gene co-expression network analysis

In order to get the better view of major chitosan response, significant expressed proteins were examined for the gene co-expression network with Rice Oligonucleotide Array Database. The locus numbers of those were used as subjects to construct the network with 0.8 cut-off value. The result revealed that there are 253 nodes and 650 edges in the co-expression network (Fig. 4.3). The main network showed that 9 loci, which were LOC_Os01g31690, LOC_Os03g03720, LOC_Os04g16680, LOC_Os04g38600, LOC_Os05g41640, LOC_Os11g47970, LOC_Os12g08730, LOC_Os12g17600, and LOC_Os12g19381, had the most positive interaction with other genes. The gene description of 9 loci was shown in Table 4.2. Besides, LOC_Os04g28180 that encoded ribosomal protein also showed the interaction with several genes, but not connected to the main network.

Table 4.2 List of major interacting proteins in chitosan response

LOC	Description
LOC_Os01g31690	Oxygen-evolving enhancer protein 1, chloroplast precursor
LOC_Os03g03720	Glyceraldehyde-3-phosphate dehydrogenase
LOC_Os04g16680	Fructose-1, 6-bisphosphatase
LOC_Os04g38600	Glyceraldehyde-3-phosphate dehydrogenase
LOC_Os05g41640	Phosphoglycerate kinase protein
LOC_Os11g47970	AAA-type ATPase family protein
LOC_Os12g08730	Thioredoxin
LOC_Os12g17600	Ribulose bisphosphate carboxylase small chain, chloroplast precursor
LOC_Os12g19381	Ribulose bisphosphate carboxylase small chain, chloroplast precursor

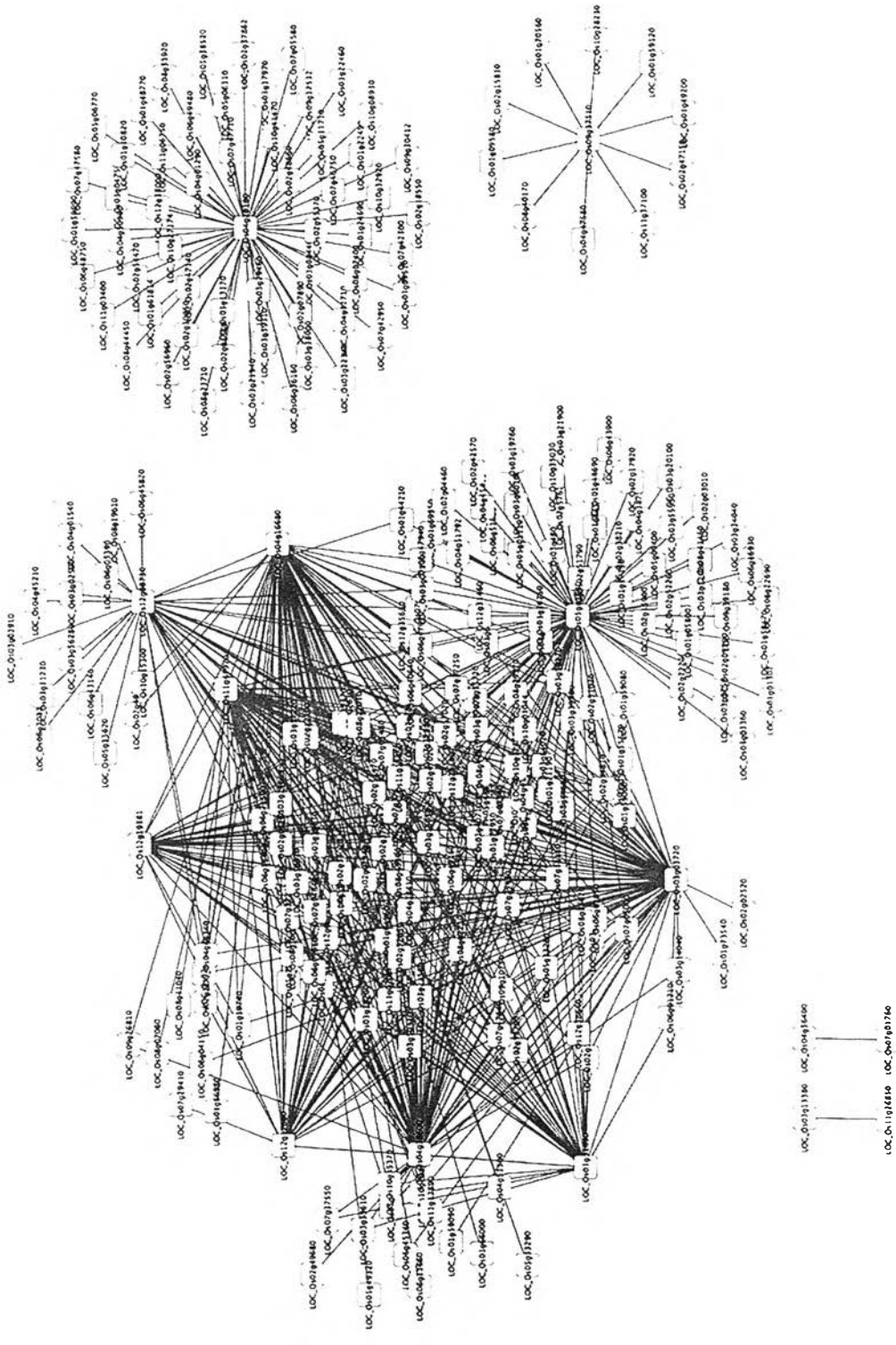

Figure 4.3 Gene co-expression network in chitosan response of 'LPT123' rice.

Chitosan is successful to elicit plant response at the protein level. Proteomic analysis of 'LPT123' rice seedlings treated with chitosan revealed the numerous protein changes mainly involved in metabolic process, signal transduction, transcription and photosynthesis.

Chitosan has been reported to activate defense response via phospholipase D- and phospholipase C-mediated signaling pathway (Raho *et al.*, 2011) as well as the up-regulation of respiratory burst oxidase to rapidly generate reactive oxygen species (ROS). ROS is a key signal transduction in the regulation of plant growth and development as well as environmental stimuli responses (Suzuki *et al.*, 2011). In contrast, excess ROS is toxic to cellular macromolecules such as lipids, protein, and DNA. H_2O_2 production was suggested to be required for chitosan induced drought tolerance in rice (Pongprayoon *et al.*, 2013). An oxidative burst or rapid H_2O_2 synthesis is a common response of plant to pathogens, elicitors, and environmental stresses. H_2O_2 acts as a messenger to induce the plant immunity gene transcription (Levine *et al.*, 1994). It is also continually generated during normal metabolism and by specific enzymes such as NADPH oxidase. In this study, respiratory burst oxidase, a subunit of NADPH oxidase was up-regulated. This protein is proposed to generate ROS during pathogen infection, response to elicitor, abiotic environment, and developmental processes (Torres and Dangl, 2005).

ROS homeostasis is crucial for attenuating the ROS toxicity and strengthening in ROS signaling. Thioredoxins are small conserved proteins that control cell redox homeostasis. They are key ROS reducers and also act as regulators of ROS scavenging mechanisms in oxidative stress response by providing electrons to peroxidoxins to remove excess ROS (Vieira Dos Santos and Rey, 2006). Thioredoxins perform a fundamental role during various steps entire plant life including photosynthesis, photorespiration, lipid metabolism, electron transport, ATP synthesis, and stress perception. Therefore, the increase of thioredoxin could be one component to protect plant cell from oxidative damage that could occur by H_2O_2 boost after chitosan application.

Based on the co-expression network analysis, thioredoxin was co-expressed with other genes involving in cell redox homeostasis such as catalase, thylakoid-bound ascorbate peroxidase and peroxisomal biogenesis factor 11 (data not showed). To balance the rate of H_2O_2 production, plants develop numerous antioxidant agents and enzymes such as ascorbic acid, glutathione, tocopherols, peroxidase and catalase (Gill

and Tuteja, 2010). Chitosan has been reported to increase peroxidase and catalase activities (Abdelbasset *et al.*, 2010). In the proteomic data, the significantly increase of peroxidase and catalase was not found between chitosan and control treatment. However, it was found the increase of thioredoxin that has not been reported to chitosan response in rice. Chitosan-raised respiratory burst oxidase and thioredoxin might indicate the activation of ROS signaling rather than toxicity in chitosan-elicited signal transduction in plant.

ATPases associated with various cellular activities (AAA) family protein was up-regulated upon chitosan activation. AAA proteins act as a chaperone that implicated in protein degradation. The main reaction are unfolding macromolecular substrates and delivering them to chambered protease for proteolysis and protein complex assembly (Hanson and Whiteheart, 2005). All substrates are degraded in ATP-dependent manner. ATP hydrolysis provides the energy for unfolding and translocation of polypeptide for degradation. AAA proteins are one of the major components of proteases and chaperones that prevent the accumulation of oxidative-damaged protein. It also protects the photosynthetic apparatus from oxidative damage occurring in the vegetative growth (Janska *et al.*, 2010).

Plant growth enhancement could require more energy supplies. Glycolysis is a crucial prominent pathway that provides fuels to plant respiration. It is a bank of numerous compounds to support macromolecule biosynthesis in the cell. Glyceraldehyde-3-phosphate dehydrogenase (GAPDH) is an enzyme that converts glyceraldehydes-3-phosphate to 1,3-bisphosphoglycerate as well as generating NADH in the sixth step of glycolysis. It also couples with phosphoglycerate kinase (PGK) to convert to 3-phosphoglycerate as well as generating ATP (Plaxton, 1996). Taken together, the increase of enolase and phosphoglucomutase might indicate more energy production supporting the numerous molecule biosynthesis for plant growth enhancement. Fructose-1,6-bisphosphatase (FBP) catalyzes an important reaction to the regeneration of ribulose-1,5-bisphosphate (RuBP) in the Calvin cycle (Ghosh *et al.*, 2001). The enhancement of these enzymes suggested that chitosan treatment stimulates plant growth enhancement via the regulation of carbon metabolism.

Photosynthesis is a process to convert light energy to chemical energy for plant growth (Taiz and Zeiger, 2006). Chitosan treatment increased photosysthetic-related proteins such as the oxygen-evolving enhancer protein 1 (OEE1) and chlorophyll a/b binding protein. These proteins function in light reaction in chloroplast. The chlorophyll a/b binding protein plays an important role in light reaction of photosynthesis. Regarding to signaling between plastids and nucleus, the control of light harvesting complex chlorophyll a/b binding protein expression is one of the mechanisms controlling the chloroplast function (Nott *et al.*, 2006). OEE1 is another protein functioning in photosystem II (PSII) complex. It is an essential for oxygen evolving activity and also considered to be the rate-limiting step in PSII assembly and stability (Sugihara *et al.*, 2000).

Not only the proteins involving in light reaction were triggered by chitosan, but also ribulose 1,5-bisphosphate carboxylase/oxygenase (RuBisCo), the key enzyme in carbon fixation was shown to be up-regulated. Ribulose bisphosphate carboxylase small chain (rbcS) which is the subunit of RuBisCo, the key enzyme in photosynthesis that play a role in the first step of carbon fixation. In plants, RuBisCo is composed of eight small subunits (SSU) and eight large subunits (LSU), which are encoded by the nuclear *rbcS* gene and the chroloplastic *rbcL* gene, respectively (Ellis, 1981). The overexpression of *rbcS* gene slightly up-regulates the gene expression of *rbcL* at the transcript level and enhances the amount of RuBisCo holoenzyme (Suzuki and Makino, 2012). This might be expected to improve the photosynthetic efficiency of chitosan-treated rice leading to the plant growth enhancement.

As the proteomics analysis showed the increase of several proteins function in chloroplasts together with the co-expression analysis data supported other chloroplast localized gene expression, it raised the idea that chloroplast is one of the target organelles for chitosan actions in plants. The photosynthetic pigment contents were previously determined in 'LPT123' rice seedlings treated with chitosan (data not showed). Chlorophyll a, chlorophyll b and carotenoid content in the chitosan treated plants were significantly higher than in the control plants. Besides, chlorophyll b/a ratio was slightly increased by chitosan. This supported the mode of chitosan action in chloroplasts and implied the improvement of photosynthesis capacity that leading to growth enhancement.

1.3 The expression of chitosan-responsive genes involving in plant growth and development

As an elicitor property of chitosan and the interest in plant growth and development, proteins from part 1.1 were selected to investigate the expression at transcription level. There were two protein annotated to be involved in signaling and also play a role in plant growth and development, LOC_Os08g25380 serine/threonine-protein kinase BRI1-like 1 precursor (*OsBRL1*) and LOC_Os06g47740 phytosulfokine receptor precursor (*OsPSKR*).

At the protein level, these two proteins were up-regulated as shown in heat map (Fig. 4.2); however, it showed the different activities at the transcription level. *OsBRL1* gene expression was decreased in both control and chitosan treatment at day 1. *OsPSKR* gene expression was increased in control treatment but decreased in chitosan treatment at day 1 (Fig. 4.4).

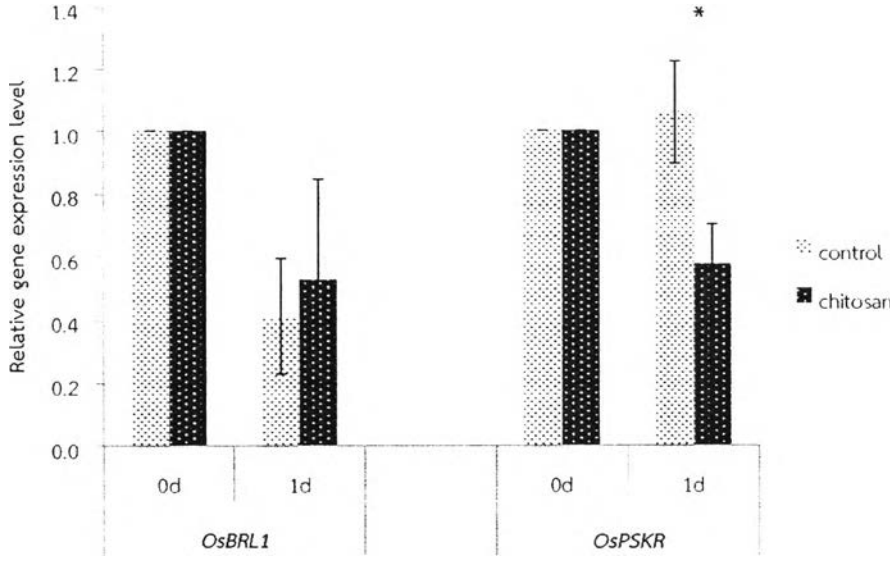

Figure 4.4 The relative gene expression level of *OsBRL1* and *OsPSKR* in 'LPT123' rice seedlings treated with or without chitosan.

Two potential receptors for plant growth induction were phytosulfokine receptor (PSKR) precursor and serine/threonine-protein kinase BRI1-like 1 (BRL1) precursor. PSKR is a receptor for phytosulfokine, a sulfated peptide promoting cellular growth of plant. The activation of PSKR affected cellular longevity without normal morphogenesis interference (Matsubayashi *et al.*, 2006). In addition, BRL1 is a homologous gene for BRI1, a brassinosteroid receptor. Normally, BRL1 strongly expressed in root but weakly expressed in leaves. It plays a role in organ development through controlling cell division and elongation but not essential for pattern formation or organ initiation (Nakamura *et al.*, 2006). Chitosan-induced PSKR and BRL1 expression in rice leaves might responsible for plant growth induction.

Although PSKR and BRL1 were increased at protein level, their gene expression patterns were not correlated. The correlation between mRNA and protein level has been reported to be typically poor. The reason might be intricate post-transcriptional mechanisms involving in mRNA translation to protein, a half live of mRNA or protein, and an error or noise of protein and mRNA experiment (Greenbaum *et al.*, 2003).

2. Identification and characterization of some chitosan-responsive genes in *Arabidopsis*

2.1 Determination of chitosan concentration for chitosan-insensitive mutant screening

Arabidopsis thaliana ecotype Columbia (Col) seeds were sterilized and grown on ½ MS medium supplemented with chitosan O80 at 0, 20, 40, 60, and 80 mg/L for 10 days. The result showed that seedling growth was inhibited by high dose chitosan in dose-dependent manner. Plant that exposed to chitosan higher than 40 mg/L showed a decreasing in plant size, root length, especially at 80 mg/L (Fig. 4.5).

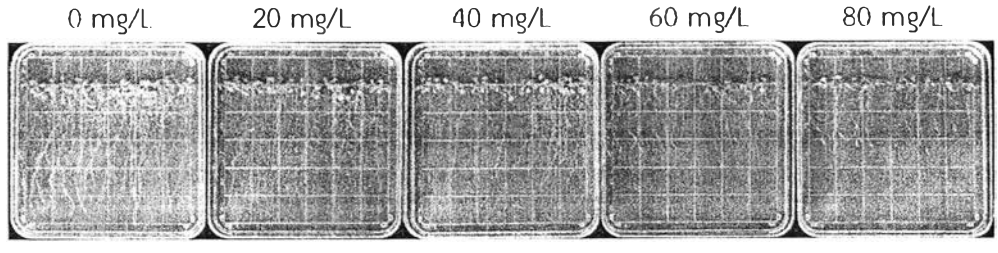

Figure 4.5 Phenotype of Arabidopsis thaliana ecotype Columbia grown on ½ MS medium supplemented with chitosan O80 at 0, 20, 40, 60, and 80 mg/L for 10 days.

Chitosan treatment higher than 50 mg/L has been reported to inhibit plant growth in term of root fresh weight and plantlet length of *in vitro* minituber of potato (Asghari-Zakaria *et al.*, 2009). The inhibition was also found in micropropagation of protocome-like body production when treated with oligomeric chitosan at 80 mg/L (Pornpienpakdee *et al.*, 2010).

Due to a large number of seeds for chitosan-insensitive (CI) mutant screening, phenotypes that easy to detect by eyes and clearly different between control (no chitosan) and chitosan treatment were selected. At 80 mg/L of chitosan, plant showed very small in plant size and about 50% shorter in root length comparing between control and chitosan treatment. This condition could be used for further screening for CI mutants.

2.2 Transcriptomic analysis of chitosan-responsive genes in *Arabidopsis*

To get further insight into the transcriptional response of *Arabidopsis* to 80 mg/L O80 chitosan, total RNA was isolated from *Arabidopsis* ecotype Col seedlings grown on ½ MS medium supplemented with or without 80 mg/L O80 chitosan. The experiment was performed in two independent biological replicates. The number of read counts for each gene obtained from Illumina sequencing and bioinformatic process directly reflected the level of its expression. Gene expression profiles of control and chitosan treatment were compared by DESeq to identify differentially expressed genes (adjusted $p<0.05$).

The results showed that chitosan treatment dramatically impacted on the transcriptome response with 1,557 genes significantly changed (see in Appendix C). The level of expression (Log_2Foldchange; Log_2FC) ranged from -4.32 to 6.25. The down- or up-regulation of genes can be indicated by negative (-4.32-0) and positive (0-6.25) values. There were 700 genes showing a down-regulation and 857 genes showing an up-regulation.

Gene ontology (GO) analysis was used to assign and classify the gene function based on TAIR10 database. Significantly expressed genes can be categorized into 15 groups (Fig. 4.6), which were metabolic process (241, 15.5%), stress (232, 14.9%), transport (128, 8.2%), regulation of transcription (97, 6.2%), development (75, 4.8%), signaling (75, 4.8%), cell wall modification (69, 4.4%), protein degradation (67, 4.3%), cell organization (54, 3.5%), secondary metabolism (50, 3.2%), photosynthesis (24, 1.5%), DNA or RNA metabolic process (17, 1.1%), and cell redox homeostasis (16, 1%), other (119, 7.7%) and unknown (294, 18.88%). In addition, the target genes were enriched in nucleus (295, 18.9%), chloroplast (214, 13.7%), and plasma membrane (214, 13.7%), respectively (Fig. 4.6).

The biological function of transcriptomic analysis is similar to data in proteomic analysis. The major changes of chitosan action involved in metabolic process and signaling processes. Taken together, chloroplast is in the second rank of cellular component of chitosan-responsive genes in *Arabidopsis*. This also supported the idea that chloroplast is one of main target organelles for chitosan actions in plants.

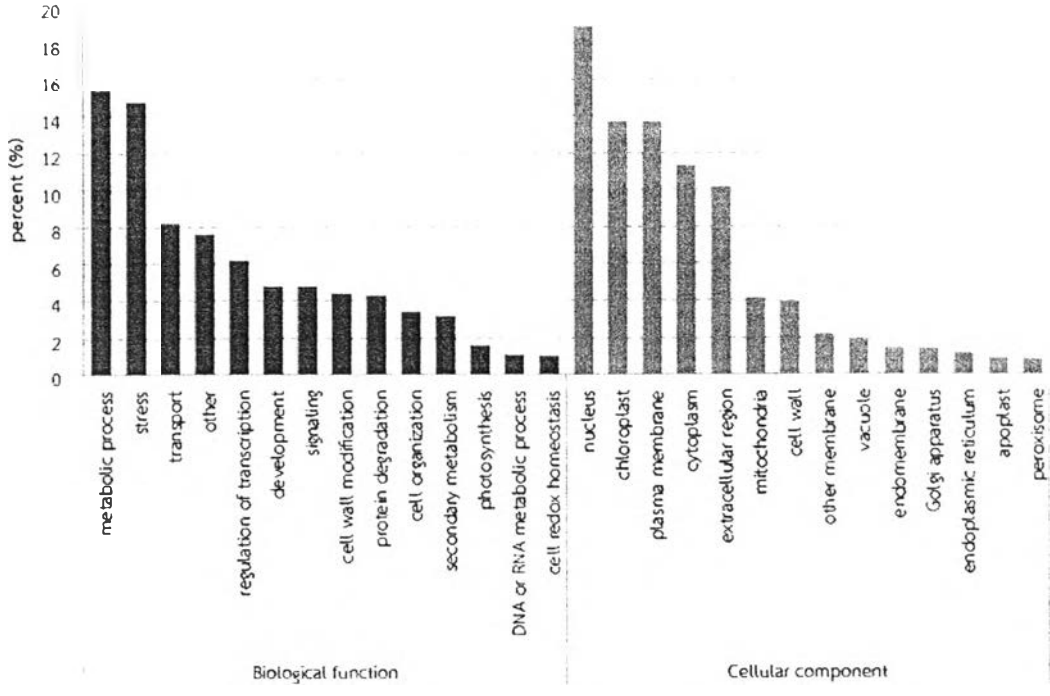

Figure 4.6 Functional categories of significantly expressed genes in *Arabidopsis* responsible for chitosan O80 at 80 mg/L. The given functions were retrieved from GO based on TAIR10 database.

2.2.1 An overview of gene co-expression network of high dose chitosan response

To provide an overview of high dose chitosan response in *Arabidopsis*, the intricate network of 1,557 chitosan-responsive genes contains 4,031 nodes with 8,743 interactions and 96 self-loops (Fig. 4.7). All Nodes were colored by SUBA subcellular localization (The SUBcellular localization database for Arabidopsis proteins). The large nodes illustrated input query genes and the small nodes illustrated interacting genes in database. The localization of query genes was mainly in nucleus, plasma membrane and chloroplast.

Due to the large number of gene interaction, the co-expression of the entire network was too complicated to interpret the high dose chitosan response at the transcriptomic level. To elucidate the gene interaction, the other gene co-expression provider was used.

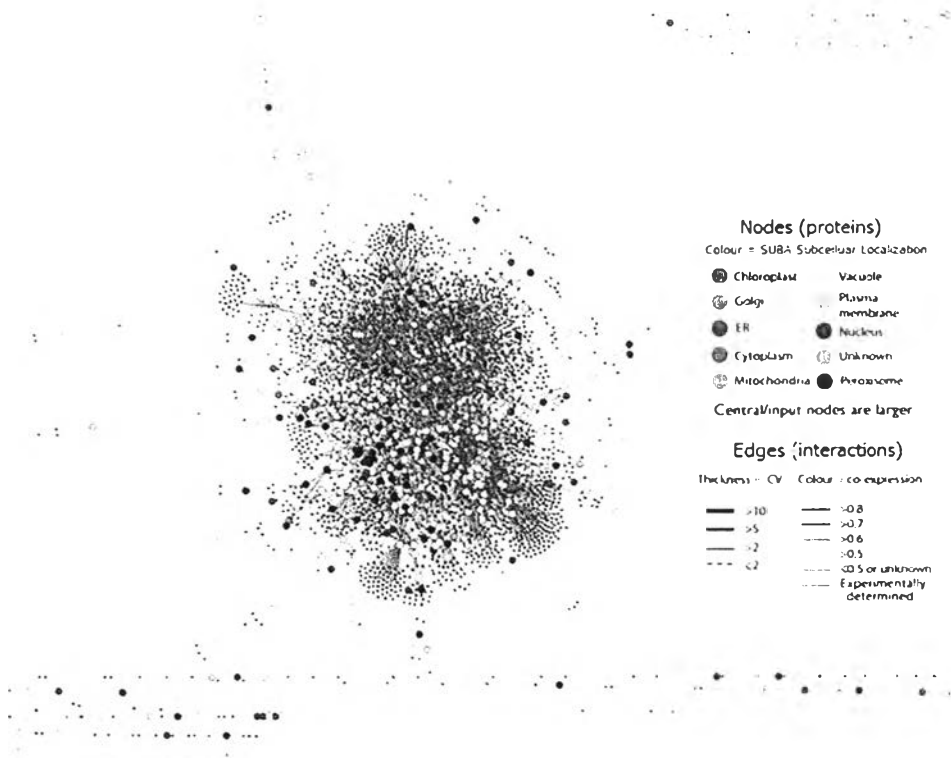

Figure 4.7 The intricate network of 1,571 chitosan-responsive genes examined by Arabidopsis Interactions Viewer in Bio-Analytic Resource database.

2.2.2 High dose chitosan disrupted growth-related gene expression

According to the adverse effects of high dose chitosan on plant growth, the groups of genes involving in plant growth and development were retrieved and analyzed using CoexSearch in ATTED-II. The results showed that all of genes involving in shoot and root development were disrupted by high dose chitosan (Table 4.3). The down-regulation of these genes could result in physiological plant growth retardation. The function of prominent genes was described below.

Table 4.3 The list of chitosan responsive genes involved in plant growth and development

Gene ID	Alias	Gene name	Log_2FC
At4g12550	AIR1	Auxin-Induced in Root cultures 1	-2.75
At4g37750	ANT	AINTEGUMENTA	-1.24
At2g01950	BRL2	BRI1-LIKE 2	-1.16
At3g50060	MYB77	MYB domain protein 77	-1.13
At1g05470	CVP2	Cotyledon vascular pattern 2	-1.05
At1g04240	IAA3	Indole-3-acetic acid inducible 3	-1.03
At4g18640	MRH1	Morphogenesis of root hair 1	-1.01
At4g24670	TAR2	Tryptophan aminotransferase related 2	-0.99
At2g02130	PDF2.3	Plant defensin 2.3	-0.95
At1g21270	WAK2	Wall-associated kinase 2	-0.85
At5g15580	LNG1	Longifolia1	-0.85
At5g51060	RHD2	Root hair defective 2	-0.84
At5g03150	JKD	JACKDAW	-0.82
At5g55730	FLA1	FASCICLIN-like arabinogalactan 1	-0.79
At3g63200	PLP9	PATATIN-LIKE PROTEIN 9	-0.78
At3g54720	AMP1	Altered meristem program 1	-0.76
At5g49270	SHV2	SHAVEN 2	-0.74
At3g04630	WDL1	WVD2-LIKE 1	-0.71
At2g22670	IAA8	Indoleacetic acid-induced protein 8	-0.65
At4g34980	SLP2	Subtilisin-like serine protease 2	-0.63
At1g52150	ATHB-15	Class III HD-ZIP protein family	-0.62
At2g34680	AIR9	Auxin-Induced in Root cultures 9	-0.61

In root system, chitosan disrupted genes involving in primary roots, lateral roots or root hair development. *ALTERED MERISTEM PROGRAM 1* (*AMP1*) encodes a putative glutamate carboxypeptidase, which is implicated in plant growth, morphogenesis and seed dormancy. It was transcriptionally down-regulated by ABA resulted in hypersensitive phenotypes toward ABA-mediated seed germination and primary root elongation. Loss-of-function of *amp1* mutant was hypersensitive to ABA with inhibited seed germination and root growth. Mutants exhibited higher level of ABA-responsive gene expression such as *RAB18*, *RD29A* and *RD29B* as well as higher concentration of proline and lower ROS levels in dehydration condition (Shi *et al.*, 2013). *AUXIN-INDUCED IN ROOT CULTURES 1* (*AIR1*) appears in lateral root development involving in the connections between the parental root cells in the lateral root growing area. *AIR1* is responsible for auxin but not other plant hormones (Neuteboom *et al.*, 1999).

MORPHOGENESIS OF ROOT HAIR 1 (*MRH1*), *ROOT HAIR DEFECTIVE 2* (*RHD2*) and *SHAVEN 2* (*SHV2*) are involved in root hair morphogenesis. *MRH1* is a leucin-rich receptor-like kinase regulated root hair tip growth. A knockout of *MRH1* results in short root hairs with normal root morphology (Jones *et al.*, 2006). *RHD2* and *SHV2* play a role in the transition from swelling formation to tip growth (Parker *et al.*, 2000). *WVD2-LIKE 1* (*WDL1*) altered normal root growth phenotypes, which is askew and wavy on tilted agar surfaces. The majority of its mutant possessed short roots that did not wave and slanted to the left on tilted agar surfaces (Yuen *et al.*, 2003). *JACKDAW* (*JKD*), a zinc finger protein, controls epidermal patterning in the root meristem that is required for appropriate expression pattern of the epidermal cell fate regulators such as *GLABRA2*, *CAPRICE* and *WEREWOLF*. It also regulates tissue boundaries and asymmetric cell division by delimiting SHORT-ROOT movement (Hassan *et al.*, 2010).

Root development can be regulated by auxin, a plant growth hormone (Estelle and Klee, 1994). Auxin-related genes were down-regulated by chitosan. *TRYPTOPHAN AMINOTRANSFERASE RELATED 2* (*TAR2*) is the auxin biosynthesis gene that required for root meristem maintenance and differential growth in apical hooks. Loss-of-function of *tar2* mutant reduces lateral root primordia emergence under low nitrogen conditions (Ma *et al.*, 2014). MYB77 is transcription factor in MYB family that interacts with auxin response factors

(ARFs) *in vitro* through the C terminus. Loss of this interaction resulted in strong reduction of lateral root numbers. In *myb77* null mutants, the auxin-responsive gene expression was dramatically attenuated (Shin *et al.*, 2007). *INDOLE-3-ACETIC ACID INDUCIBLE 3* (*IAA3*) is a member of auxin-induced Aux/IAA gene family. *IAA3* regulated auxin-dependent root growth, lateral root formation, and timing of gravitropism (Tian and Reed, 1999). *FASCICLIN-like arabinogalactan 1* (*FLA1*) is a member in the family of arabinogalactan-proteins (AGPs). It is regulated in an auxin-dependent pathway as a primary hormone response gene. It was implicated to plays a role in initial stage of both lateral root and shoot development. Mutant of *fla1* also showed defects in shoot regeneration (Johnson *et al.*, 2011).

In shoot system, the retardation of plant growth was also affected by organ size, cell elongation, and vascular development. *AINTEGUMENTA* (*ANT*) controls intrinsic plant organ size by regulating plant organ cell number and extending cell division throughout shoot development (Mizukami and Fischer, 2000) (Yuen *et al.*, 2003). *LONGIFOLIA1* (*LNG1*) regulates longitudinal cell elongation by controlling polar cell elongation rather than cell proliferation. The *lng1* mutant showed decreased leaf length associated with less longitudinal polar cell elongation (Lee *et al.*, 2006). *COTYLEDON VASCULAR PATTERN 2* (*CVP2*) encodes inositol polyphosphate 5'-phosphatases that generates the specific phosphoinositides (PIs) ligand. The binding of specific PIs regulated the sorting of vesicle cargos to discrete cellular sites in yeast and animal cells. In Arabidopsis, specific PIs control the vesicle traffic that is essential for polarized and continuous vein pattern formation (Carland and Nelson, 2009).

BRI1-like (*BRL*) was showed to be up-regulated in proteomic analysis of rice seedlings in the condition of plant growth induction. The contrary effect of high dose chitosan on plant growth, *BRL2* in *Arabidopsis* was inhibited. BRL2 is a receptor-like kinase (RLKs) belonging to BRI1 family. It plays a role in vascular development restricted to provascular and procambial cells for venation formation. It interacts with vascular-specific adaptors, tetratricopeptide repeat (TPR)-containing proteins (*At1g04770* and *At3g51280*), which were also down-regulated. The disruption of *BRL2* and interacting genes has showed defects in vein pattern and changing in auxin and brassinosteroids responses (Ceserani *et al.*, 2009).

Furthermore, other RLKs involving in plant growth and development were found in the transcriptomic data. High dose chitosan inhibited *CLAVATA1* (*CLV1*) and CLAVATA1-related receptor (*BAM2*) gene expression (see in gene list in Appendix C). *CLAVATA1* (*CLV1*) is a regulator that maintains cell proliferation in shoot apical meristems in *Arabidopsis*. It plays a role in cell division patterns and cell-cell signaling. *CLV1* malfunction disrupted of leaf development. CLV1 has been reported to physically interact with CLAVATA1-related receptor, BAM1. CLV1 or CLV1/BAM1 complexes are the prominent regulators of stem cells in shoot meristems. (Durbak and Tax, 2011). Otherwise, the interaction between CLV1 and BAM2 has not been reported. CLAVATA1-related receptor called Barely Any Meristem 2 (BAM2) functions in multiple developmental pathways from shoot to floral development and is required for proper stem cell maintenance. *BAM* genes play complementary or opposite developmental roles to *CLV1* within the meristem in term of the reduction in meristem size, meristem termination and reduction in floral organs observed in *bam* mutants (DeYoung *et al.*, 2006) However, the repression of *CLV1* and *BAM2* could suggest the disruption of meristem development that required for proper plant growth in the vegetative stage.

2.2.3 Chitosan influenced in photosynthetic system, chlorophyll breakdown and iron homeostasis

Photosystem I and II as well as electron transport chain were directly interrupted by high dose chitosan (Table 4.4). The target genes included two photosystem II reaction center (*PSBH* and *PSBM*), two light harvesting complex (*LHCB2.4* and *LHCB4.3*), one photosystem I reaction center (*PSAN*). In addition, two ferritins (*FER3* and *FER4*), which encode iron storage protein (Tarantino *et al.*, 2010), were affected by chitosan.

Chlorophyll is a key player for light energy harvesting in light reaction in photosynthesis (Taiz and Zeiger, 2006). One of photosynthesis-disrupting factors could be a degradation of chlorophylls by removing chlorophylls from thylakoid membranes and breaking down to colorless compound in multiple-step pathways. This process was catalyzed by chlorophyllase, and pheophytinase (Aiamla-or *et al.*, 2012). Transcriptomic analysis showed that two chlorophyllase (*CLH1* and *CLH2*) and *pheophytinase* (*PPH*) were up-regulated by high dose chitosan (Table 4.4).

Chlorophyllase catalyzes the hydrolysis of chlorophyll to chlorophyllide and phytol. *CLH1* is rapidly induced after tissue damage and by pathogen attack. It has been proposed to be a plant damage controller and modulate the balance between different plant defense pathways including systemic acquired resistance (SAR) (Kariola *et al.*, 2005). *Pheophytinase* (*PPH*) is an important component in an early chlorophyll breakdown during senescence. *PPH* is involved in the dephytylation of pheophytin to pheophorbide but does not accept chlorophyll as substrate (Schelbert *et al.*, 2009). In addition, pheide a oxygenase (PaO) is specific for senescence-induced chlorophyll breakdown. It is a nonheme iron type monooxygenase that degrades pheide a during senescence. *Accelerated cell death 1* (*ACD1*) is identical to *AtPaO* in *Arabidopsis* (Pruzinska *et al.*, 2003). The increase of *CLH, PPH, and ACD1* might indicate chlorophyll breakdown induced by both SAR and senescence.

Iron is required for photosynthetic composition and chlorophyll content. The disruption of iron homeostasis regulators gene expression leads to change of proper photosynthesis and chlorophyll activities. The result showed that high dose chitosan triggered the gene expression involved in iron homeostasis such as *FER-like regulator of iron uptake* (*FIT1*), *ferric reduction oxidase 2* (*FRO2*), and *vacuolar iron transporter family protein* (*VIT*) as well as *FER3* and *FER4* in photosynthesis process (Table 4.4).

In the absence of *ferritins*, plants had higher level of ROS together with increasing ROS detoxifying enzyme activities. *FER4* is an iron storage protein that controls intraorganellar iron trafficking (Tarantino *et al.*, 2010). *FER4* was reported to have a partial inverse relationship of transcript level of *FRO3*, which was up-regulated in high dose chitosan treatment. *FIT1* encodes a putative transcription factor regulating iron homeostasis. Its mRNA is detected in the outer root cell layers and responses to iron deficiency. *FIT1* regulates the expression of more than 40% of iron-deficiency-inducible genes and is essential for normal plant growth and development under iron sufficient conditions. *FIT1* regulated *FRO2*, the rate-limiting step in iron acquisition, at the transcription level (Colangelo and Guerinot, 2004). *FRO2* transcript level coordinately rises in roots imposition of iron deficiency and coordinately declines following iron re-supplement (Kerkeb *et al.*, 2008). Iron localization in provascular strand required the proper *VIT* expression which is not dependent to iron availability in soil. VIT1 involves in vacuolar iron influx involved in intracellular metal transport and are also important for maintaining iron homeostasis that critical for seedling development (Kim *et al.*, 2006).

On the other hand, two FIT-independent iron-regulated transcription factors, *bHLH100* and *bHLH101*, were up-regulated. *bHLH100* and *bHLH101* play a crucial role in iron-deficiency responses. Their mutants showed severe defect phenotypes in growth and iron homeostasis when growing on low-iron media. They play a non-redundant role with the FIT-dependent bHLH factors such as *bHLH038* and *bHLH039* (Sivitz *et al.*, 2012).

Table 4.4 The list of chitosan responsive genes involved in chlorophyll breakdown, photosynthesis and iron homeostasis

Category	Gene ID	Alias	Gene name	Log_2FC
Chlorophyll breakdown	At1g19670	CLH1	Chlorophyllase 1	1.47
	At5g43860	CLH2	Chlorophyllase 2	1.16
	At5g13800	PPH	Pheophytinase	1.13
	At3g44880	ACD1	Accelerated cell death 1	1.23
Photosynthesis	At2g40300	FER4	Ferritin4	-2.26
	At5g10170	MIPS3	Myo-inositol-1-phosphate synthase 3	-1.48
	At2g40100	LHCB4.3	Light harvesting complex of photosystem II	-1.10
	At3g27690	LHCB2.4	Photosystem II light harvesting complex gene 2.3	-1.06
	At4g26530		Fructose-bisphosphate aldolase 5	-1.05
	At5g64040	PSAN	Photosystem I reaction center subunit PSI-N	-0.97
	Atcg00220	PSBM	Photosystem II reaction center protein M	-0.97
	At3g56090	FER3	Ferritin 3	-0.91
	Atcg01010	NDHF	NADH dehydrogenase unit F	-0.90
	Atcg00710	PSBH	Photosystem II reaction center protein H	-0.86
	Atcg01110	NDHH	NAD(P)H dehydrogenase subunit H	-0.71
	Atcg00180	RPOC1	RNA polymerase beta' subunit-1	-0.67
	Atcg00730	PETD	Photosynthetic electron transfer D	-0.66
	Atcg01050	NDHD	NAD(P)H dehydrogenase complex	-0.64
	At3g15840	PIFI	Post-illumination chlorophyll fluorescence increase	0.82
	At1g64810	APO1	Accumulation of photosystem one 1	0.95
Iron homeostasis	At2g28160	FIT1	FER-like regulator of iron uptake	-1.25
	At1g01580	FRO2	Ferric reduction oxidase 2	-0.67
	At1g23020	FRO3	Ferric reduction oxidase 3	0.92
	At3g25190	VIT	Vacuolar iron transporter family protein	-2.00

2.2.4 Chitosan action on nutrient uptake

To provide an energy source for transport of nutrients into the cell, plasma membrane H^+-ATPase is an electrogenic enzyme generating an electrochemical gradient and proton driving force. It generates a membrane potential that could drive nutrient transport system both cation and anion such as K, Ca, Mg, NH_4, NO_3, PO_4, and SO_4 (Palmgren, 2001).

High dose chitosan increased plasma membrane H^+-ATPase (*AHA3*) that has been reported to response to pathogen-associated molecular patterns (PAMPs) (Elmore and Coaker, 2011) and *ATPase E1-E2 type family protein* (*At3g27870*), which has not been reported. High dose chitosan dramatically triggered several nutrient transport systems both cation and anion. The highest negative influences were on potassium transporter (*HAK5*) (Nieves-Cordones *et al.*, 2010), sulfate transporter (*SULTR3;5*) (Kataoka *et al.*, 2004) , *ammonium transporter 1;3* (*AMT1;2* and *AMT1;3*) (Yuan *et al.*, 2007), nitrate transporter (*NRT1.1*) (Remans *et al.*, 2006), and zinc transporter (*ZIP2* and *ZIP3*) (Grotz *et al.*, 1998). In the other hand, the highest positive influences were on nitrate transporter (*NRT1.7*, *NRT1.8*) (Li *et al.*, 2010), calcium exchanger 7 (*CAX7*) and cation exchanger 3 (*CAX3*) (Maser *et al.*, 2001) (see in Appendix C). The alterative appearance of nutrient transport systems supported the large amount of rearrangement of metabolic process in chitosan response.

2.2.5 Cell wall modification

Cell wall is an important barrier for plant exposing to unfavorable condition. The barriers include pectin composition, cell wall cross-linking and cell wall proteins and chemicals (Cosgrove, 2005; Kempema *et al.*, 2007). High dose chitosan treatment influenced cell wall modification mostly in the negative direction (see in Appendix C). For example, *expansin* (*EXPA*), implicated in the rapid extension or stress relaxation of cell wall (Cosgrove, 2000), pectin modification (e.g. *pectate lyase, pectin methylesterase, pectinesterase*), and *arabinoglycan protein* (*AGP*). Besides, chitosan also affected secondary cell wall modification such as callose (*CALS1*), which is responsive to chitosan treatment (Franco and Iriti, 2007) and lignin biosynthesis (*CAD*) (Van Acker *et al.*, 2013) and catabolic process (*LAC*) (Turlapati *et al.*, 2011). Lignin is assembled by oxidative polymerization of coniferyl alcohol and sinapyl alcohol. Laccases have been proposed to be involved in lignin synthesis by catalyzed the polymerization of the monolignol alcohols. Disruption of *laccase* genes only leads to a change in lignin content and only under continuous illumination. The earlier lignification could inhibit root elongation (Cachorro *et al.*, 1993). *Laccase* genes have been reported to be involved in normal growth and development regulation and response to osmotic stress (Liang *et al.*, 2006). Besides, *casparian strip membrane domain proteins* (*CASP1* and *CASP2*) were inhibited by high dose chitosan (see in Appendix C). Casparian strip is formed by lignin and suberin deposition (Schreiber *et al.*, 1999). The alteration of lignin content might affect the decrease of *CASP* gene expression.

2.2.6 Chitosan activates biotic/abiotic stress responses

Giving an importance to biotic/abiotic stress responses, chitosan-responsive genes were also investigated using MapMan (Thimm *et al.*, 2004). The 1,557 significantly expressed genes and their log_2FC were subjected to MapMan. Genes were mapped in biotic stress pathway based on TAIR10 database. The result indicated that chitosan had an influence on biotic stress responses including pattern recognition receptors (PRRs), pathogen-related (PR) proteins, transcription factors, hormone signalling, and secondary metabolites as well as several abiotic stress responsive genes (Fig. 4.8).

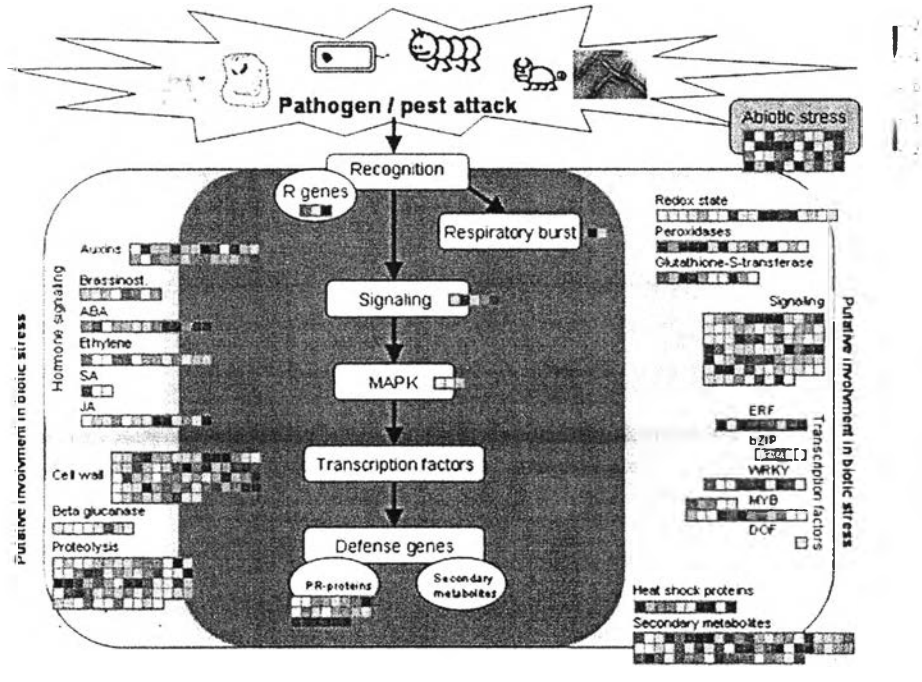

Figure 4.8 Mapman display of biotic/abiotic stress genes responsive to high dose chitosan. Red color indicated gene induction and blue color indicated gene repression.

2.2.6.1 Pattern recognition receptors (PRRs)

Plant innate immunity was activated by PRRs that mostly located on the plasma membrane of cells. PRRs could be receptor-like kinases (RLKs), receptor-like protein kinases (RLPs), elongation factor-Tu (EF-Tu) receptor, and lectin receptor (Barre *et al.*, 2002; Zipfel, 2008). High dose chitosan triggered the expression of PRRs at transcription level. RLPs (*RLP1*, *RLP6* and *RLP40*), cysteine-rich RLKs (*CRK11*, *CRK13*, *CRK14*, and *CRK22*), lectin receptor (*LECRKA4.1* and *HLECRK*) and EF-Tu receptor (*EFR*) were up-regulated (see in Appendix C). In addition, the receptor responsive to fungal pathogen was induced, *Botrytis-induced kinase1* (*BIK1*) (see in Appendix C; Eckardt, 2011). Plant RLPs and RLKs have been reported to detect a broad range of PAMPs such as *RLP1* responsive to *Xanthomonads* (Jehle *et al.*, 2013), *CRK13* responsive to *Pseudomonas syringae* (Acharya *et al.*, 2007). The increase of known bacterial responsive receptor like *EFR* (Zipfel *et al.*, 2006) and *LECRKA4.1* (Riou *et al.*, 2002) also illustrated the appearance of PAMP-triggered responses found in chitosan actions. Contrastly, high dose chitosan decreased *RLP12*, *RLP29*, *CRK4*, *CRK25*, Receptor-like kinase (*RKL1*), and LysM domain-containing receptor (*LYK4*) (see in Appendix C). *CRK4* has been reported to trigger salicylic acid (SA)-induced hypersensitive response-like cell death in overexpressing transgenic plants (Chen *et al.*, 2004). The decrease of *CRK4* expression seems to suggest that SA-induced cell death might not occurred in high dose chitosan response. Other RLPs and RLKs has not been reported for their function in PAMP responses. *LYK4* is important for chitin signaling and plant innate immunity in *Arabidopsis* (Wan *et al.*, 2012). The *LYK4* down-regulation might suggest the divergence of signaling between chitin and chitosan.

2.2.6.2 Pathogenic and biotic stress responsive genes

A large number of pathogen-responsive genes were up-regulated by high dose chitosan such as plant defensins (*PDF1.2A, PDF1.3,* and *PDF1.4*) (Manners *et al.*, 1998; Germain *et al.*, 2011; Meng *et al.*, 2013), tyrosine aminotransferase (*TAT3*) (Povero *et al.*, 2011), polygalacturonase inhibiting protein (*PGIP1* and *PGIP2*) (O'Brien *et al.*, 2012), PR genes (i.e. *beta-1,3-glucanase 2* (*BGL2*), *pathogenesis-related 4* (*PR4*), and *chitinase* (*CHI*)) (Agrios, 2005), camalexin production (GSTF6) (Su *et al.*, 2011). Secondary metabolite biosynthesis was also increased including anthocyanin (*MYB75/PAP1* and *TT18/ANS*) (Stracke *et al.*, 2007) and terpenes (*TPS04* and *LAS1*) (Barah *et al.*, 2013).

2.2.6.3 Abiotic stress responsive genes

Chitosan also strongly induced stress-responsive genes including heat, cold, and osmotic stress, for example, heat shock proteins (HSPs) (*HSP21, HSP17.6II, HSP17.4,* and *HSP70B*) (Carvalho *et al.*, 2012), cold responsive (COR) regulons (*COR6.6*, *COR15a*, *KIN1*) (Chinnusamy *et al.*, 2007), CBL-interacting protein kinase (*CIPK3*, *CIPK5*, *CIPK21*, *CIPK9*, and *CIPK25* except *CIPK15*, a negative regulator of ABA signaling) (Yoon *et al.*, 2009), responsive to dessication (*RD20*, *RD22*, *RD26*, *RD29A* and *RD29B*) (Abe *et al.*, 2003; Wang *et al.*, 2011), early-responsive to dehydration (*ERD5*) (Rossel *et al.*, 2007), proline biosynthesis (*P5CS1* and *P5CS2*) (Szekely *et al.*, 2008), and senescence-related genes (*SEN1*) (Schenk *et al.*, 2005). Mitogen-activated protein kinase (MAPK or MPK) was implicated in common signaling cascade translator for external stimuli. High dose chitosan induced *MPK7* gene expression. MPK7 is activated by H_2O_2 but not bacterial flagellin (flg22) (Dóczi *et al.*, 2007). This might suggest that plant defense and stress responses activated by high dose chitosan probably partially diverse from flg22 signaling.

2.2.6.4 Reactive oxygen species (ROS) homeostasis

Hydrogen peroxide (H_2O_2) and nitric oxide (NO) are known to produce in response to chitosan elicitation. It was found that oxidative burst regulator, aspartate oxidase (AO), was down-regulated. AO catalyzes the first irreversible step in the *de novo* NAD biosynthesis and required for NADPH-mediated oxidative burst (Macho *et al.*, 2012). This might lead to the suppression of oxidative burst-related genes such as *NADPH oxidase*, *RBOHC/RHD2*, respiratory burst oxidase, *CDS2*, *FSD1*, and *PRX33*. Furthermore, *nitrite reductase 1* (*NIR1*) that necessary for NO production was also suppressed (Desikan *et al.*, 2002). Oxidative burst is rapid and transient ROS production. It is induced by oligogalacturonides (OGs) but not required for the activation of OG-induced defense responses (Galletti *et al.*, 2008). These probably suggested that oxidative burst might not be required in high dose chitosan response with the long period. However, high dose chitosan induced the ROS scavenging systems, which were *catalase 1* (*CAT1*), *glutathione peroxidase* (*GPX1*, *GPX7*), and *dehydroascorbate reductase* (*DHAR5*) together with thioredoxin and glutaredoxin (Rouhier *et al.*, 2008; Foyer and Noctor, 2009; Szechynska-Hebda and Karpinski, 2013). Nevertheless, *stromal ascorbate peroxidase* (*SAPX*) was down-regulated. The increase of these enzymes could be a consequence of ROS produced from another pathway such as metabolic process, plant physiological processes or biotic/abiotic stress responses (Quan *et al.*, 2008).

2.2.6.5 Plant hormone biosynthesis and signaling

According to Mapman display, chitosan had influences on plant hormone such as abscisic acid (ABA), jasmonic acid (JA), and ethylene (ET). For better understanding the hormone regulation, additional hormone-related genes were retrieved from ATTED-II and literature reviews. Chitosan has been implicated to be pathogen-mimicking stimulus. The alteration of hormone regulation possibly behaved as in pathogen response. ABA and JA appear to play a prominent role in response to high dose chitosan supporting by the increase of gene expression in their biosynthesis, catabolism, signaling and responses. List of prominent genes was showed in Table 4.5.

Table 4.5 The list of prominent chitosan-responsive genes involved in hormone signaling

Category	Pathway	Gene ID	Alias	Gene name	Log_2FC
ABA	Biosynthesis	At3g14440	NCED3	Nine-cis-epoxycarotenoid dioxygenase 3	1.68
		At2g27150	AAO3	Abscisic aldehyde oxidase 3	1.18
	Catabolism	At3g19270	CYP707A4	Cytochrome P450, family 707, subfamily A, polypeptide 4	1.64
		At4g19230	CYP707A1	Cytochrome P450, family 707, subfamily A, polypeptide 1	1.04
		At5g45340	CYP707A3	Cytochrome P450, family 707, subfamily A, polypeptide 3	-1.04
	Signaling and response	At5g66400	RAB18	Responsive to ABA 18	4.33
		At1g07430	HAI2	Highly ABA-induced PP2C gene 2	2.48
		At5g59220	HAI1	Highly ABA-induced PP2C gene 1	2.28
		At1g15520	PDR12	Pleiotropic drug resistance 12	1.67
		At5g57050	ABI2	ABA insensitive 2	1.28
		At1g72770	HAB1	Homology to ABI1	1.10
		At4g26080	ABI1	ABA insensitive 1	0.91
		At3g19290	ABF4	ABRE binding factor 4	0.83
		At4g33950	OST1	Open stomata 1	0.78
		At5g15960	KIN1	Stress-responsive protein	3.54
		At2g39800	P5CS1	Delta1-pyrroline-5-carboxylate synthetase 1	1.93
		At3g55610	P5CS2	Delta1-pyrroline-5-carboxylate synthetase 2	0.77

Category	Pathway	Gene ID	Alias	Gene name	Log_2FC
JA	Biosynthesis	At3g25760	AOC1	Allene oxide cyclase 1	2.35
		At3g25770	AOC2	Allene oxide cyclase 2	1.29
		At1g17420	LOX3	Lipoxygenase 3	1.08
		At5g42650	AOS	Allene oxide synthase	0.95
		At2g06050	OPR3	Oxophytodienoate-reductase 3	0.63
	Catabolism	At3g48520	CYP94B3	Cytochrome P450, family 94, subfamily B, polypeptide 3	2.41
	Signaling and response	At2g24850	TAT3	Tyrosine aminotransferase 3	4.70
		At5g13220	JAZ10	Jasmonate-zim-domain protein 10	2.35
		At5g06870	PGIP2	Polygalacturonase inhibiting protein 2	2.07
		At3g57260	BGL2	Beta-1,3-glucanase 2	1.61
		At1g19670	CLH1	Chlorophyllase 1	1.47
		At1g70700	JAZ9	Jasmonate-zim-domain protein 9	1.26
		At1g17380	JAZ5	Jasmonate-zim-domain protein 5	1.08
		At5g06860	PGIP1	Polygalacturonase inhibiting protein 1	1.08
		At1g19180	JAZ1	Jasmonate-zim-domain protein 1	0.97
		At3g17860	JAZ3	Jasmonate-zim-domain protein 3	0.83
		At5g20900	JAZ12	Jasmonate-zim-domain protein 12	0.76
		At1g74950	JAZ2	Jasmonate-zim-domain protein 2	0.75
		At2g40750	WRKY54	WRKY DNA-binding protein 54	-1.34
		At3g56400	WRKY70	WRKY DNA-binding protein 70	-1.42
ET	Biosynthesis	At4g26200	ACS7	1-Amino-cyclopropane-1-carboxylate synthase 7	1.20
		At2g19590	ACO1	ACC oxidase 1	-1.07
	Signaling	At5g61600	ERF104	Ethylene response factor 104	-0.70
AUX	Biosynthesis	At3g44300	NIT2	Nitrilase 2	2.58
		At4g24670	TAR2	Tryptophan aminotransferase related 2	-0.99
CK	Biosynthesis	At3g63110	IPT3	Isopentenyltransferase 3	-1.20

ABA plays important roles in plant growth development and stress responses. The ABA actions are controlled by the precise balance between its biosynthesis and catabolism. High dose chitosan stimulated genes in ABA biosynthesis (*AAO3*, *NCED3*) (Finkelstein and Rock, 2002) and catabolism (*CYP707A1, 3* and *4*) (Kushiro *et al.*, 2004). The ABA actions in chitosan-elicited transcriptome response is also supported by the up-regulation of genes in ABA signaling and responses, for example, regulator of ABA signaling (*HAI1* and *HAI2*) (Bhaskara *et al.*, 2012; Zhang *et al.*, 2013), a plasma membrane ABA uptake transporter (*PDR12*) (Kang *et al.*, 2010)

and ABA-inducible genes (*RAB18* (Hallouin *et al.*, 2002), *ABF4* (Wang *et al.*, 2011)). Chitosan has been reported to induce stomatal closure (Lee *et al.*, 1999). Open stomata 1 (*OST1*) is a positive regulator of ABA actions implicated in stomatal closure. It is regulated by ABA level and negative regulators of ABA (*ABI1* and *ABI2*). Stomata of *ost1* mutant failed to close in response to ABA but not effected to open stomata in response to light (Kushiro *et al.*, 2004). The up-regulation of *OST1* and *ABI* might be a part of chitosan actions in stomatal closure.

JA controls plant development and plant defense and also known as wound hormone. High dose chitosan induced genes involved in JA biosynthesis (Schaller and Stintzi, 2008), which were *LOX3*, *AOS*, *AOC1*, *AOC2*, *OPR3*, and *ACX1* as well as JA catabolism (*CYP94B3*). CYP94B3 controlled jasmonoyl-L-isoleucine (JA-Ile) turnover. CYP94B3 converts JA-Ile to 12OH-JA-Ile (12-hydroxy-JA-Ile). 12OH-JA-Ile is less effective than JA-Ile to promote the formation of COI1-JAZ receptor complexes. CYP94B3 actions in negative feedback control JA-Ile levels and performs a key role in attenuation of jasmonate responses (Koo *et al.*, 2011).

ET is involved in many plant processes through their life cycle such as root hair development and senescence. Although one ethylene biosynthesis gene, *ACS7*, was induced, the key step enzyme to convert ACC to ethylene, *ACO1* (Wang *et al.*, 2002), was inhibited. ACS7 was implicated to be involved in ABA and stress responses. The induction of ACS7 in high dose chitosan treatment might result from ABA biosynthesis and stresses (Dong *et al.*, 2011).

Auxin (AUX) and cytokinin (CK) are known to regulate plant growth and development including requirement of proper plant root development. High dose chitosan negatively affected on AUX and CK biosynthesis. For AUX biosynthesis genes, *NIT2* was induced whereas TAR2 was suppressed. *NIT2* encodes a nitrilase, which converts IAN to auxin. It was induced by diverse stresses (Huh *et al.*, 2012). This suggested that the increase of *NIT2* might result from high dose chitosan-mimicking stresses. *TAR2* was reported to express in the mature root zone near the root tip (Ma *et al.*, 2014). As adverse effect of high dose chitosan on plant root, the decrease of *TAR2* might be because of the retarded root growth and

development. In addition, AUX influx and efflux carriers (*ABCB19*, *PIN1*, *PIN5*, *LAX3*, and *LAX2*) were also inhibited (Mravec *et al.*, 2009; Titapiwatanakun *et al.*, 2009; Vandenbussche *et al.*, 2010; Sawchuk *et al.*, 2013). It also found that CK biosynthesis gene (*IPT3*) was down-regulated. Besides, auxin-induced physiological appearance can be antagonized by OGs via inhibition of auxin-responsive gene expression. The repression of auxin responses in *Arabidopsis* not only detected in OGs response but also in bacteria elicitor flagellin especially at high dose of elicitor (Savatin *et al.*, 2011).

2.2.6.6 Transcription factors

Transcription factors are the regulators for gene expression. High dose chitosan induced or repressed several transcription factors in different families including ERF, MYB, NAC and WRKY families. The changing of transcription factors gene expression might be consequences of biotic/abiotic stress response and alteration of plant growth development that occurred upon chitosan treatment. The reported functions of genes were indicated below.

In *Arabidopsis*, most of WRKY genes respond to pathogen and stress stimuli. High dose chitosan induced eight WRKY transcription factors. *WRKY6* and *WRKY22* trigger signal transduction pathways in plant senescence and defence responses (Robatzek and Somssich, 2001; Zhou *et al.*, 2011). *WRKY15* modulates plant growth against salt/osmotic stress (Vanderauwera *et al.*, 2012). *WRKY25* and *WRKY26* enhance heat tolerance ability and act as positive regulators of HSPs-related signaling pathways (Li *et al.*, 2011). *WRKY28* is strongly induced by H_2O_2 and required for resistance to *Botrytis cinerea* (Wu *et al.*, 2011). *WRKY45* was induced by ozone treatment (Tosti *et al.*, 2006). *WRKY48* is induced by stress and pathogen acting as a negative regulator of basal defense for the *Pseudomonas syringae (Xing et al., 2008).* In contrast, only two WRKYs were repressed. *WRKY54* and *WRKY70* are co-operative as negative regulators of leaf senescence responding to SA but not to H_2O_2 (Besseau *et al.*, 2012). The decrease of *WRKY54* and *WRKY70* suggested the occurring of senescence in plant exposed to high dose chitosan.

MYB transcription factors play a role in plant growth development, abiotic stress tolerance and hormone signaling. Fourteen MYB and MYB-like was affected by high dose chitosan. Seven MYBs were induced. *MYB13* was also induced by *Botrytis* infection (AbuQamar *et al.*, 2006). *MYB15*, an ABA-responsive gene, involves in osmotic stress tolerance (Ding *et al.*, 2009). *MYB47, MYB94* and *MYB112* were responsive to ABA and abiotic stress (Singh *et al.*, 2011; Ding *et al.*, 2013). *MYB75* is a transcription factor in sucrose-mediated anthocyanin biosynthesis (Teng *et al.*, 2005), and *MYBL2* is a new regulator of flavonoid biosynthesis (Dubos *et al.*, 2008). While, the other seven MYBs were down-regulated. *MYB51* is a transcription factor essential for MAMP-elicited callose deposition

(Millet *et al.*, 2010). *MYB77* is a modulator of auxin-inducible genes in lateral root formation (Shin *et al.*, 2007). *MYB73* is involved in the function against *Bipolaris oryzae (Jia et al., 2011)*. *MYB88* is a transcription factor in stomatal development (Lai *et al.*, 2005). The other *MYBs* (*MYB93*, *MYB124*, and *MYB3R-4*) have not been previously reported the functions.

NAC transcription factors are key regulators not only in stress perception but also in plant development. Nine NACs were up-regulated upon high dose chitosan treatment. *ATAF1* is a negative regulator of defense response against pathogens (Wang *et al.*, 2009). *NAC019* and *NAC55* are implicated to enhance senescence (Hickman *et al.*, 2013). *NAC029* negatively affects salicylic acid signaling (Penfold and Buchanan-Wollaston, 2014). *NAC089* is up-regulated by endoplasmic reticulum stress (Yang *et al.*, 2014). The other *NACs* (*NAC6*, *NAC044*, *NAC047*, and *NAC102*) have not been previously reported the functions. Whereas, only *NAC36* was down-regulated.

AP2/ERF transcription factor family plays a role in phytohormone, pathogen and environmental stress responses. High dose chitosan induced transcription factors that related to AP2 (RAP) i.e. *RAP2.3*, *RAP2.10*, *RAP2.6*, *RAP2.6L (Sakuma et al., 2002)*, while *ERF104*, a flg22-regulated basal immunity regulator was repressed (Bethke *et al.*, 2009).

2.2.7 A comparison of transcriptional profiling between previous study and high dose chitosan study revealed different responses of chitosan elicitation

Previous study of microarray-based transcriptional profiling of chitosan-responsive genes was investigated in 4-day-old *Arabidopsis* treated with chitosan at 150 mg/L for 3 h (Povero *et al.*, 2011). This study, *Arabidopsis* were grown on ½ MS medium with or without 80mg/L chitosan for 10 days. The comparison revealed that 19.65% (306 of 1557) of chitosan-responsive gene loci were similar (Fig 4.9, Appendix C).

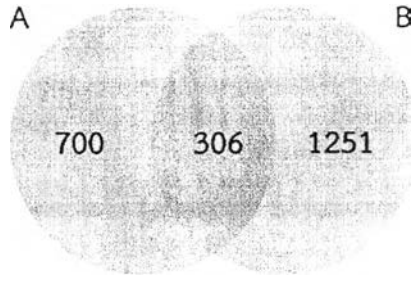

Figure 4.9 Venn diagram of the overlap between genes differential regulated by chitosan in two studies. A: Povero's study, B: this study.

The overlapped genes were mainly implicated in plant defense and stress responses. The gene expression mostly showed in the same direction with varied different level. In this study, ABA inducible receptor, lectin-receptor kinase, LRRs, CRKs, and RLPs showed less level of induction as well as the lower level of downstream gene expression. Only two genes involved in amino acid metabolic process (*threonine aldolase 1*; *THA1* and *glutamine-dependent asparagine synthetase 1*; *ASN1*) and two hormone responsive genes (*RAB18* and *AOC1*) were higher.

The others showed the opposite direction of gene expression. In this study, *MYB51*, *WAK1*, *ERF104*, *pathogen and circadian controlled 1* (*PPC1*) and *disease resistance protein (TIR-NBS class)* genes were repressed. Whereas, all heat shock proteins were induced. An overlap of a few chitosan-responsive genes and the different level of gene expression suggested that the different complex signal transduction was elicited by chitosan with different source, concentration, and time of treatment leading to divergence of plant responses.

2.3 EMS-mutagenesis *Arabidopsis* seed preparation

At least 3,000 Col seeds were mutagenized by 25 mM EMS and grown on soil to produce M_2 seeds. After 2 months of growing, seeds were pooled from 5 to 10 M_1 plants. Seeds were kept in dark and dry place at room temperature until screening.

2.4 Screening of chitosan-insensitive mutagenized *Arabidopsis*

At least 120,000 M_2 plants have been screened for CI mutants by examining plant phenotype on the chitosan selective medium for 10 days. Several phenotypes of mutagenized seedlings were broadly detected. Most of them showed dwarf phenotype that could be observed by eyes, for example, small leaf, short hypocotyls, small cotyledons, and short roots. It also showed a high number of no germination and albino plants. This indicated the efficiency of the EMS mutagenesis (Bernå *et al.*, 1999).

After the first screening, about 350 putative mutants showed the CI phenotypes by comparing plant size or root length to wild-type plant. The putative M_2 mutants were transferred from medium agar plate to soil in an individual pot. Mutants were grown for another 2 months to obtain M_3 seeds. For soil-grown plants, the putative M_2 mutants showed varying in leaf shapes including normal as wild-type plant and various leaf formation abnormality. Leaf shape of mutants can be categorized into phenotypic classes defined by Bernå *et al.* (1999 as shown in Table 4.6.

Table 4.6 Leaf phenotypic classes of chitosan-insensitive *Arabidopsis* according to definition by Bernå *et al.* (1999)

Phenotypic class	Leaf phenotype of each class
Denticulata (Den)	Pointed lamina with dentate margins
Elongata (Elo)	Narrow and elongated lamina and long petiole
Rotunda (Ron)	Broad and rounded lamina
Scabra (Sca)	Rounded and protruded lamina
Ultracurvata (Ucu)	Lamina spirally rolled downward
Dentata (Dea)	Serrated margins
Incurvata (Icu)	Involute margins
Transcurvata (Tcu)	Margin obliquely revolute

Incidentally, about 40 putative M_2 mutants died prior completing theirs life cycles, had an early senescence, had no flower or were sterile. These lines could not go through further steps.

M_3 seeds from the remaining putative M_2 plants were separately collected for CI mutant screening. Wild-type and M_3 seeds were surface-sterilized and vertically grown on ½ MS medium with 0 or 80 mg/L of chitosan for 10 days. During the screening, some putative mutants showed retarded growth when exposed to chitosan but less than occurred in wild-type plants. The effects varied in different lines, for example, mutants grew better than wild-type plant in normal condition, but grew worst or equal to wild-type plant in chitosan condition.

Plant phenotype responsible for chitosan can be separated into 3 categories as show in Table 4.7. Category 1, mutant plant showed higher growth than wild-type plant in normal condition (+/++) and showed less retard growth in chitosan condition (--/-). Category 2, mutant plant showed normal growth same as wild-type plant in normal condition (+/+) and showed less retarded growth in chitosan condition (--/-). Category 3, mutant plant showed normal growth same as than wild-type plant in normal condition (+/+) and showed more retarded growth in chitosan condition (-/--). In the last category, it might be because the homozygous mutation occurs in the lethal genes in *Arabidopsis* genome in M_3 generation (Budziszewski *et al.*, 2001).

Table 4.7 Phenotype categories of wild type and mutant in the second screening

Category	Normal condition		Chitosan condition	
	Wild type	Mutant	Wild type	Mutant
1	+	++	--	-
2	+	+	--	-
3	+	+	-	--

+ represents normal growth

++ represents higher growth

- represents less retard growth than wild type

-- represents more retard growth than wild type

In M_3 generation, other leaf defect phenotypes were also observed. Coloration of mutant leaf varied from normal green to darkened green, pale green or purple leaves. Pale-green-leaf M_3 plants previously showed CI phenotype and normal green color in their M_2 generation. A week after germination, lots of mutant lines showing pale-green leaf could not show the insensitive phenotype. It was growing worst when compared with wild-type plant under chitosan condition. Additionally, leaf of a few mutants turned to be darkened or purple. They also showed less CI phenotype than in their M_2 generation.

Finally, five putative mutant lines, 21I, 86B, 106A, 129A, and 161A were obtained (Fig. 4.10). Phenotype of the putative mutant was showed in Table 4.8. The other weak CI phenotype mutant lines were showed using line 39A (Fig. 4.10F) as a representative.

Table 4.8 Phenotypes of the putative mutants

Mutant line	Phenotypes	Figure
21I	Bigger in plant size and longer roots	Fig. 4.10A
86B	Bigger in plant size and longer roots	Fig. 4.10B
106A	Slightly longer roots	Fig. 4.10C
129A	Slightly longer roots	Fig. 4.10D
161A	Bigger in plant size and slightly longer roots	Fig. 4.10E

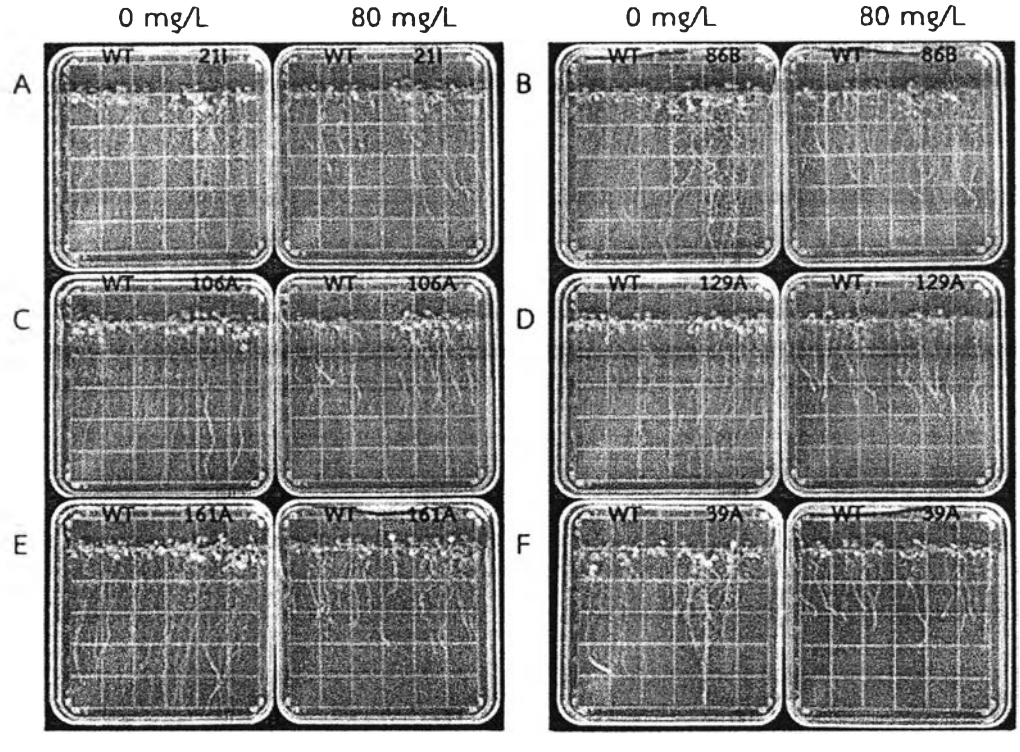

Figure 4.10 Phenotype of putative CI mutant. A: 21I; B: 86B; C: 106A; D: 129A; E: 161A; F: 39A. (left plate: 0 mg/L of chitosan; right plate: 80 mg/L of chitosan).

2.5 Genetic inheritance analysis by test cross with Landsberg *erecta* (L*er*)

M_3 individuals from these remaining 5 lines were testcrossed to mapping lines, Col or L*er*, to determine the inheritance pattern of mutated gene in F_1 and F_2 progeny. Crosses between mutants and wild-type plant were achieved by transferring pollen from mutant to stigma of emasculated flowers of wild-type plant.

Firstly, the testcross of M_3 individuals were done with commonly used background line, Landsberg *erecta* (L*er*). However, heterosis was found in a hybrid offspring of wild type (L*er* x Col). Hybrid plants slightly grew better than their parents (Col or L*er*) such as an increase in plant size and root length or more lateral roots (Fig. 4.11). These characters dramatically confound the CI phenotypes that we used for the screening.

To solve the problem, testcross within Col was substituted to avoid the confounding effect of hybridization to L*er*. It was very important with genes that have a relatively subtle effect. The testcross for all 5 lines was done before knowing that the heterosis effect of L*er* x Col confound the insensitive phenotype. While waiting for a production of Col cross, the pattern of inheritance of F_2 population of mutants in L*er* cross was investigated. This might roughly screen for genetic inheritance pattern of putative mutants.

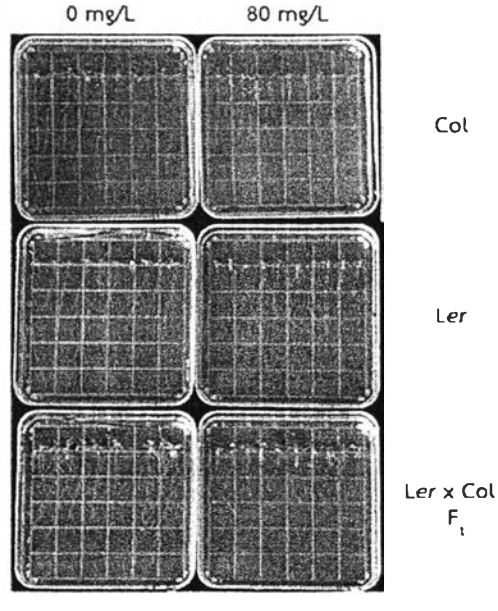

Figure 4.11 Phenotype of wild-type Arabidopsis Col, L*er* and F_1 hybrid of L*er* x Col.

Within L*er* cross, all F_1 progeny had short root phenotype, which similar to phenotype of wild-type plant when exposed to high dose chitosan. The segregation ratio of the short root: long root phenotype was observed as shown in Table 4.9. F_2 progeny of L*er* x 21I and L*er* x 86B showed the segregation ratio of 10:1 and 24:1, respectively. On the contrary, F_2 of the others showed the segregation ratio of short root: long root phenotype as 3:1. Not only the longer root phenotype was found in these 3 mutant lines, the larger shoot was also detected under 80 mg/L chitosan supplement.

Two more testing for line 129A, 106A and 161A were performed to confirm the stability of the insensitive phenotype. It was found the 129A line showed inconsistent phenotype, while 106A and 161A lines performed consistently long root on chitosan-supplemented medium.

Table 4.9 Root phenotype of F_1 and F_2 progeny (L*er* cross) on the ½ MS medium supplemented with 80 mg/L chitosan

Cross	F_1 phenotype	F_2 phenotype (segregation ratio)
L*er* x 21I	Short roots	Short roots/ long roots (10:1)
L*er* x 86B	Short roots	Short roots/ long roots (24:1)
L*er* x 106A	Short roots	Short roots/ long roots (3:1)
L*er* x 129A	Short roots	Short roots/ long roots (3:1)
L*er* x 161A	Short roots	Short roots/ long roots (3:1)

2.6 Genetic inheritance analysis by test cross with Col

In order to eliminate the heterosis effects of L*er* background, 106A and 161A lines were crossed with Col-ecotype *Arabidopsis*. Approximately 300 seeds of each F_2 progeny were grown on chitosan-supplemented medium to investigate the genetic segregation. If the insensitive phenotypes are regulated by a single recessive gene, plants will have short roots: long roots phenotype as 3:1 in F_2 progeny. After the crosses, F_2 progeny of 106A x Col and 161A x Col showed the segregation short roots: long roots as 3:1. Therefore, these two lines could be used for further characterization.

2.7 Identification of EMS-induced mutation by Next-Generation Sequencing

A recessive pool of F_2 progeny of 106A and 161A lines was selected by long root phenotype. About 50 plants of each F_2 family were pooled and the genomic DNA was isolated for genomic library preparation and sequencing. Two genomic DNA libraries were sequenced on one lane using Illumina's Genome Analyzer II (50-bp single-end reads). Reads from Illumina sequencing were processed in a bioinformatic pipeline for sequence alignment with BWA (version 0.7.3a) and SAMtools (version github-1.18). The obtained sequences were mapped to *Arabidopsis* reference genome TAIR10.

After sequence analysis, the list of candidate genome positions with associated mutational effects was obtained. It was analyzed by SnpEff program to predict the effects of variants on genes such as Single-Nucleotide Polymorphism (SNPs), multiple-nucleotide polymorphism (MNPs) and insertion-deletion (In-del) in the whole genome sequences. Annotated genes can be classified into synonymous or non-synonymous SNPs, stop codon gains or losses etc. To determine which mutation are actually damaging, we evaluated the probability of an amino acid substitution that affects protein function using SIFT Blink as described in methods. The prediction based on the degree of amino acid residues conservation in sequence alignments from closely related sequences through PSI-BLAST (Kumar *et al.*, 2009). Proteins that have the normalized probability for an amino acid substitution or SIFT score ≤ 0.05 were predicted to be damaged. Putative mutation in each mutant line was showed in section 4 in Appendix D. The candidate status was determined by SIFT score and the percentage of occurrence base mutation in the genomic DNA sequencing data (data not showed).

2.8 Mutant ordering and confirmation

Candidate mutated genes in each mutant line were searched for T-DNA insertion mutants with Col background in germplasm or seed stock in Arabidopsis Biological Resource Center (ABRC). Nine germplasms were found and their seeds were ordered from ABRC for the following characterization (Table 4.10).

Table 4.10 List of T-DNA insertion mutants ordered from ABRC

Mutant line	No.	Gene ID	Gene name	Stock #	Insertion position
106A	1	At1g04160	Myosin XI B	SALK_113062C	Chr1: 1088453
	5	At4g08470	MAPK/ERK kinase kinase 3	SALK_093491C	Chr4: 5385369
	6	At2g02180	Tobamovirus multiplication protein 3	SALK_020637	Chr2: 560972
	7	At1g01250	DREB subfamily A-4 of ERF/AP2 transcription factor family	SALK_044673	Chr1: 104559
	8	At5g64410	Oligopeptide transporter 4	SALK_055333	Chr5: 25755491
161A	2	At1g18040	Cyclin-dependent kinase D1;3	SALK_007756C	Chr1: 6207130
	3	At1g72920	Toll-Interleukin-Resistance (TIR) domain family protein	SALK_081457C	Chr1: 27437915
	4	At1g16780	Type II H+-PPases that localizes to and function as a proton pump of the Golgi apparatus	SALK_085653C	Chr1: 5744286
	9	At1g54780	Thylakoid lumen protein 18.3	SALK_077808	Chr1: 20439318

No.: Assigned number for ABRC mutant lines

Insertion position: T-DNA insertion in genomic DNA (chromosome number: position)

T-DNA insertion mutants ordered from ABRC were assigned number as in Table 4.10. It was grown on soil in an individual pot to produce seeds for characterization and PCR confirmation. Leaf tissues of soil-grown mutants were collected and frozen immediately in liquid nitrogen for further DNA and RNA extraction. Seeds of mutants were collected one by one plant.

2.8.1 Confirmation of T-DNA insertion in ABRC mutants

Specific primers for PCR confirmation were retrieved from T-DNA Primer Design by using Stock# (SALK_number) as a query (see primer sequence in Appendix D). Genomic DNA from leaf tissues of soil-grown mutants were isolated and used as template in PCR. The amplification condition was as described in materials and methods. The principle of PCR detection of T-DNA insertion in mutant was described in SIGnAL (Salk Institue Genomic Analysis Laboratory; http://signal.salk.edu/tdnaprimers.2.html)

The result showed that PCR product illustrated the existence of T-DNA insertion except line 9 (Fig. 4.12). ABRC mutant line 1, 2, 4 and 8 are homozygous mutants (indicated by the existence of only lower band) and line 3, 5, 6 and 7 are heterozygous mutants (indicated by the existence of both upper and lower band).

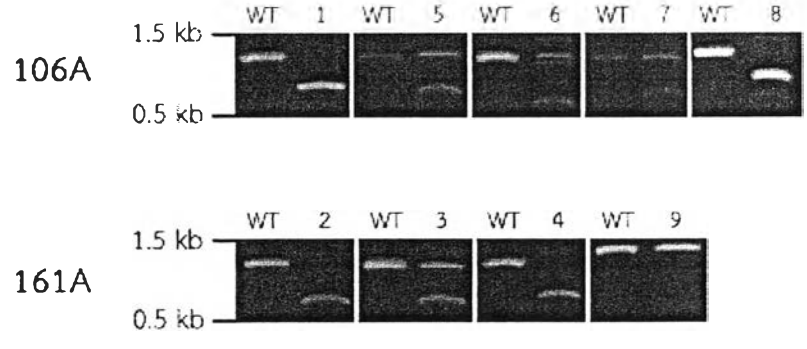

Figure 4.12 PCR confirmation of ABRC mutant to detect T-DNA insertion in genomic DNA.

2.8.2 Investigation of the level of RNA in ABRC mutant by RT-PCR

Gene-specific primers for RT-PCR detection were designed manually and confirmed with OligoAnalyzer and primer-BLAST tool in NCBI (see primer sequence in Appendix D). Total RNA from leaf tissues of soil-grown mutants was isolated and cDNA were synthesized as described in materials and methods and used as template in PCR. The amplification condition was as described in materials and methods.

The result showed that PCR product illustrated the lower expression of mutated gene in line 1, 2, 5 and 8. The comparable level was detected in line 3, 4 and 7. The gene expression was not detected in both line 6 and wild-type plant (Fig. 4.13).

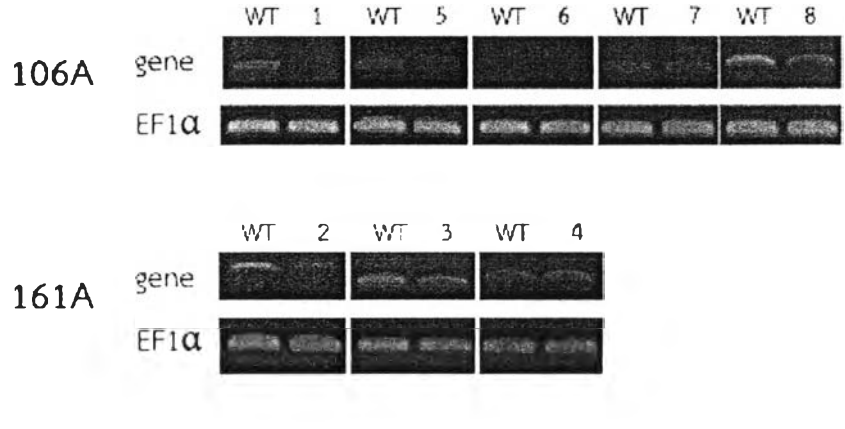

Figure 4.13 RT-PCR of ABRC mutant to detect the level of RNA.

2.9 Characterization of ABRC mutants responding to high dose chitosan

Arabidopsis mutants harboring T-DNA insertion ordered from ABRC were grown on ½ MS medium with or without chitosan (Fig. 4.14). In normal condition (0 mg/L chitosan) ABRC mutants grew similarly to wild-type plant. In chitosan condition, most of them grew as similar as wild-type plant except line 6 and 8, which carry mutation in *tobamovirus multiplication protein 3* (*TOM3*) and *oligopeptide transporter 4* (*OPT4*), respectively. These two genes might be a part of high dose chitosan responses, while the others might not be a part of these responses. However, the better growth seemed not to significantly difference.

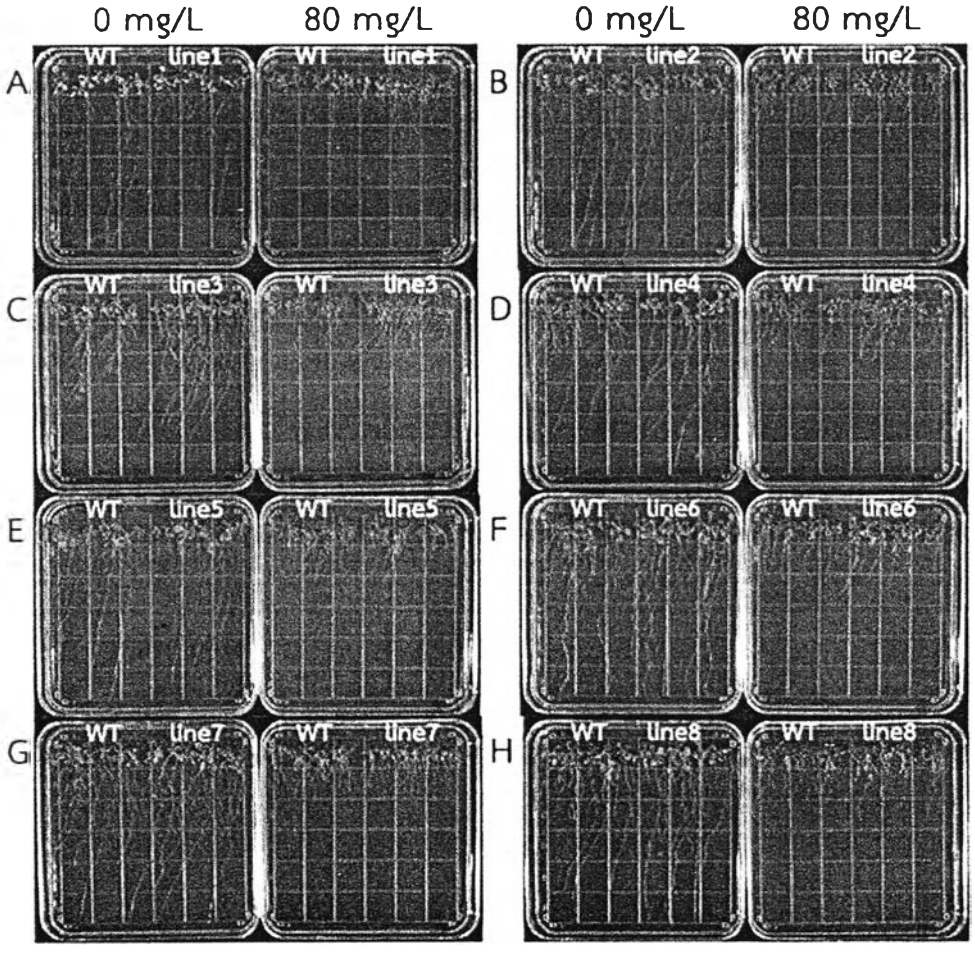

Figure 4.14 Phenotype of wild-type plant and ABRC mutants grown on ½ MS medium with or without chitosan. Letter A to H indicated ABRC mutant line 1 to line 8. (left plate: 0 mg/L of chitosan; right plate: 80 mg/L of chitosan).

2.9.1 The information of tobamovirus multiplication protein (TOM)

The understanding of *TOM3* function has not been elucidated. They only characterized the role of *TOM3* in multiplication of the tovamovirus. Loss of *TOM3* alone does not affect the complete inhibition of tobamovirus multiplication (Fujisaki *et al.*, 2006). It would require more information to explain the role of *TOM3* in chitosan response. As its response to virus infection, the level of *TOM3* might not be detected in wild-type plant (Fig 4.13, line6).

2.9.2 The information of oligopeptide transporter (OPT)

Oligopeptide transport is the process of translocation of small peptides (2–6 residues in length) across the cellular membrane required energy in a dependent manner. Oligopeptide transporter (OPT) is a proton-coupled high-affinity transporter for oligopeptides. OPT is able to transport glutathione derivatives and some metal complexes under sulfur-deficient condition and may be involved in stress resistance. In *Arabidopsis*, OPT has been reported to involved in embryo development, peptide signaling in stress response (Stacey *et al.*, 2002; Pike *et al.*, 2009). Expression analysis of *OPT* indicated that *OPTs* involved in nitrogen mobilization during germination and senescence, pollen tube growth, pollen and ovule development, seed formation and metal transport (Stacey *et al.*, 2006). The interesting point is iron-deficiency does not affect the expression of *AtOPT1, 4, 6, 7,* and *8* under limiting-iron availability (Stacey *et al.*, 2006), which occurred in high dose chitosan response. These might be the point that *opt4* mutant slightly grew better than wild-type plant under high dose chitosan supplement.

2.10 Gene comparison between RNA-seq and CI mutant experiment

When comparing the locus number of obtained genes from RNA-seq and CI mutant data, none of identical locus number was found. However, oligopeptide transporter and Toll-Interleukin-Resistance (TIR) domain family protein were found in both experiments with different locus number. In RNA-seq experiment, the level of *TIR domain family protein* was down-regulated, whereas *oligopeptide transporter (OPT1)* was up-regulated. In CI mutant experiment, ABRC mutant carrying insertion in *TIR domain family protein* did not show the high dose chitosan insensitivity (Fig. 4.14C), whereas the mutant carrying insertion in *OPT4* slightly showed the insensitivity to high dose chitosan (Fig. 4.14H). These might support the function of *OPT* in chitosan responses.

3. Identification of ortholog gene(s) involving in chitosan responses in rice

The lists of chitosan-responsive genes obtained from step 2 both RNA-seq and chitosan-insensitive (CI) mutant screening were used as identifiers to find rice orthologous genes using Rice DB.

3.1 Identification of rice orthologous genes comparing to RNA-seq

When using RNA-seq data as an identifier, the results of 1,314 rice orthologous genes were found, but 243 identifiers were not found. Locus numbers of these genes were compared to data from proteomic approach. Only 9 rice orthologous genes were identical, which were *LOC_Os10g0272*, *LOC_Os09g15330*, *LOC_Os10g31780*, *LOC_Os03g52070*, *LOC_Os08g01150*, *LOC_Os08g44910*, *LOC_Os03g18640*, *LOC_Os08g39550*, and *LOC_Os01g12680* (detail as in Table 4.11).

Table 4.11 List of rice orthologous genes comparing between RNA-seq and proteomic data

Gene ID	Alias	Gene name	LOC	Gramene identity score(%)
At1g21250	WAK1	Cell wall-associated kinase	LOC_Os10g02720	28%
At1g77210	STP14	Sugar transport protein 14	LOC_Os09g15330	69%
At3g04000		NAD(P)-binding Rossmann-fold superfamily protein	LOC_Os10g31780	46%
At3g10450	SCPL7	Serine carboxypeptidase-like 7	LOC_Os03g52070	31%
At3g61270		Unknown protein	LOC_Os08g01150	39%
At4g14465	AHL20	AT-hook motif nuclear-localized protein 20	LOC_Os08g44910	47%
At5g07130	LAC13	Laccase 13	LOC_Os03g18640	57%
At5g12940		Leucine-rich repeat (LRR) family protein	LOC_Os08g39550	54%
At5g24030	SLAH3	SLAC1 homologue 3	LOC_Os01g12680	44%

More than a half of the orthologous genes showed the opposite direction of gene expression. Only 4 genes were similar, which were *sugar transport protein 14* (*STP14*), *NAD(P)-binding Rossmann-fold superfamily protein* (*At3g04000*), *Serine carboxypeptidase-like 7* (*SCPL7*), and *SLAC1 homologue 3* (*SLAH3*). Of which, *STP14* has the highest identity score. *STP14* is a galactose transporter whose expression regulated by many factors involved in cell wall degradation and sugar level (Poschet *et al.*, 2010).

3.2 Identification of rice orthologous genes comparing to predicted gene mutation

When using predicted gene mutation as an identifier, the result showed 7 orthologous genes, but 2 identifiers were not found. *LOC_Os02g34080*, *LOC_Os02g57190* and *LOC_Os03g64290* were orthologous with *myosin XI B*. *LOC_Os05g32600* and *LOC_Os05g32600* were orthologous with *cyclin-dependent kinase D-1;3*. *LOC_Os02g33490* was orthologous with *type II H+-PPases*. *LOC_Os02g53030*, *LOC_Os02g53040*, *LOC_Os03g15570*, *LOC_Os03g49640*, and *LOC_Os03g49640* were orthologous with *MAPK/ERK kinase kinase 3*. *LOC_Os03g02850*, *LOC_Os03g02850*, and *LOC_Os10g39220* were orthologous with *tobamovirus multiplication protein 3*. *LOC_Os01g43940*, *LOC_Os02g46850*, *LOC_Os02g46860*, and *LOC_Os04g50820* were orthologous with *oligopeptide transporter 4*. *LOC_Os05g33280* was orthologous with *thylakoid lumen protein 18.3*.

Locus numbers of these genes were compared to data from proteomic approach. None of them were identical to data from proteomic approach. However, only one similar gene group was found, *STE_MEKK_ste11_MAP3K*. Mitogen-Activated Protein Kinase Kinase Kinases (MAPKKKs or MAP3Ks or MEKKs) are important components of MAPK signaling cascades and play important role in plant growth and development. The roles of MAP3K have been identified in various stresses, innate immunity and defense responses, plant cytokinesis, and hormone signaling. *MAP3K* gene family in rice is poorly elucidated. Information about proving to be bottleneck in MAPK cascade is very important monocot crop. In rice genome databases, a total of 75 *MAP3K* genes were identified and of which 70 genes were novel (Rao *et al.*, 2010). However, mutant carried *MAP3K* insertion did not show the insensitivity of high dose chitosan response. It might not be the key component in chitosan elicitation, but involved in the subsequence responses of its action.